Phenotiki: An open software and hardware platform for affordable and easy image-based phenotyping of rosette-shaped plants

Phenotiki: An open software and hardware platform for affordable and easy image-based phenotyping of rosette-shaped plants

Massimo Minervini [1], Mario Valerio Giuffrida [1,2,3], Pierdomenico Perata [4], Sotirios A. Tsaftaris [1,2]

[1] Pattern Recognition and Image Analysis (PRIAn), IMT School for Advanced Studies, Piazza S. Francesco 19, 55100 Lucca, Italy

[2] Institute for Digital Communications, School of Engineering, University of Edinburgh, Thomas Bayes Road, EH9 3FG, Edinburgh, UK

[3] The Alan Turing Institute, British Library, 96 Euston Road, NW1 2DB, London, UK

[4] PlantLab, Institute of Life Sciences, Scuola Superiore Sant'Anna, Via Mariscoglio 34, 56124 Pisa, Italy

To whom correspondence should be addressed:

Sotirios A. Tsaftaris
Tel: +44 (0)131 650 5796
E-mail: s.tsaftaris@ed.ac.uk

Running title: Phenotiki: Affordable phenotyping of rosette plants

Keywords: phenotyping, computer vision, Arabidopsis thaliana, growth, software, image analysis, affordable, Raspberry Pi.

Word count: Total = 7435. Summary (247), Introduction (669), Results (2847), Discussion (1888), Experimental Procedures (1296), Acknowledgments (82), Figure Legends (406). References (1424).

Summary

Phenotyping is important to understand plant biology but current solutions are either costly, not versatile or difficult to deploy. To solve this problem, we present Phenotiki, an affordable system for plant phenotyping which, relying on off-the-shelf parts, provides an easy to install and maintain platform, offering an out-of-box experience for a well established phenotyping need: imaging rosette-shaped plants. The accompanying software (with available source code) processes data originating from our device seamlessly and automatically. Our software relies on machine learning to devise robust algorithms, and includes automated leaf count obtained from 2D images without the need of depth (3D). Our affordable device (~200€) can be deployed in growth chambers or greenhouses to acquire optical 2D images of approximately up to 60 adult Arabidopsis rosettes concurrently. Data from the device are processed remotely on a workstation or via a cloud application (based on CyVerse). In this paper, we present a proof-of-concept validation experiment on top-view images of 24 Arabidopsis plants in a combination of genotypes that has not been previously compared. Their phenotypic analysis with respect to morphology, growth, color and leaf count has not been done previously comprehensively. We confirm findings of others on some of the extracted traits showing that we can phenotype at reduced cost. We also perform extensive validations with external measurements and with higher fidelity equipment and find no loss in statistical accuracy when we use the affordable setting we propose. Device setup instructions and analysis software are publicly available (http://phenotiki.com).

Significance statement

Phenotyping is important to understand plant biology but current solutions are costly, not versatile and difficult to deploy. Here, we present an affordable and easy to deploy phenotyping platform with publicly available software performing a well established plant phenotyping task: quantify rosette growth, morphology, color, and leaf count from images acquired by a device and analyzed remotely on workstations or in the cloud.

INTRODUCTION

The plant research community appreciates the need to phenotype fast and in a reliable fashion the growth of plants. Having an in-depth understanding of such information could help us identify suitable traits to be utilized for breeding new crops. Model plants, such as *Arabidopsis thaliana*, combined with quantitative information obtained manually or via observation, have become an invaluable tool in this quest (Furbank and Tester, 2011). Recently, the introduction of digital imaging and automation have radically changed how phenotypes are described (Rousseau et al., 2015) in model plants and in general. Experts can analyze the images offline (i.e., at a later point in time after the actual plant experiment), disentangling the process of imaging (sensing) from phenotype analysis. With image analysis, this process has been further simplified (Sozzani et al., 2014) and the labor effort has been significantly reduced to the point that automated phenotyping is now sought-after by many laboratories around the world in an attempt to relieve the phenotyping bottleneck (Furbank and Tester, 2011).

As a result, several phenotype acquisition approaches have emerged which can be broadly categorized as those relying on commercial equipment (for example made by LemnaTec [http://www.lemnatec.com], CropDesign [http://www.cropdesign.com], Phenospex [http://phenospex.com], Photon Systems Instruments [http://www.psi.cz]) or custom-built solutions that may rely on affordable (e.g., Tsaftaris and Noutsos, 2009, and Bours et al., 2012, De Vylder et al., 2012; Green et al., 2012; Leister et al., 1999) or costly imaging sensors coupled with actuation (Apelt et al., 2015; Brown et al., 2014; Granier et al., 2006; Jansen et al., 2009; Tisné et al., 2013; Walter et al., 2007). Both approaches have a key limitation: high barrier to entry, either due to cost or difficult deployment and maintenance or lack of a robust and expandable software platform. This has hindered the widespread adoption of image-based technologies as a practical and standard tool in plant phenomics for the common lab.

In this paper we propose *Phenotiki*, an affordable and yet practical approach to phenotyping of rosette-shaped plants that is easy to install and deploy and is accompanied by robust, free (with available source code) software.

Phenotiki (cf. Figure 1) combines an imaging device but also a complete, open, expandable standalone software (cf. Figure S3) designed to offer an out-of-box experience when used together. To be affordable (less than 200€), easy to deploy, use and maintain, no moving parts are used and all hardware is easy to source as it is based on the Raspberry Pi platform. The software system offers automated or semi-automated analysis of several visual phenotypes, based on a wide range of traits ranging from typical size and growth descriptors to color and even leaf count. Our imaging device is tasked with taking images, and we offer software that runs on the device to enable easy programmatic control. Analysis (and data storage) occur at local workstations or via the web browser in the cloud. Our analysis software, to be reliable when used in different laboratories (or even with other imaging systems), integrates analysis algorithms centered in state-of-the-art methods of image processing and machine learning that have appeared in engineering conferences and journals passing the technical scrutiny of the audience of these venues (Giuffrida et al., 2015; Minervini et al., 2014; Minervini et al., 2015a). Notably, we include machine learning driven methods for: (i) automated plant segmentation from tray images (Minervini et al., 2014); (ii) semi-automated interactive leaf segmentation (Minervini et al., 2015a); and (iii) automated leaf counting (Giuffrida et al., 2015), all within the confines of affordable 2D-based vision without the need for costly 3D cameras (Apelt et al., 2015).

To demonstrate the phenotyping potential of Phenotiki, we present results from a proof-of-concept experiment containing several replicates of Arabidopsis (wild-type and mutants) that were imaged simultaneously. We characterized the accuracy of the system with traditional manual measurements and other (costlier) imaging sensors. Several statistical experiments on extracted growth, morphological, and color phenotypes confirmed that Phenotiki can phenotype at a remarkably reduced cost.

RESULTS

Plant Material

The experiment involved 24 *Arabidopsis thaliana* plants, including the wild-type (ecotype Col-0) and four different mutants, all in Col-0 background, with an arrangement as shown in Figure 2b. The *constitutive triple response 1* (*ctr1*; Kieber et al., 1993) and *ethylene insensitive 2* (*ein2.1*; Guzmán and Ecker, 1990) are defective in ethylene signaling. The *pgm* mutant is unable to accumulate transitory starch as a consequence of a mutation in the plastidic isoform of the phosphoglucomutase (*PGM*), which is required for starch synthesis (Caspar et al., 1985). The *adh1* mutant is defective in alcohol dehydrogenase activity, an enzyme playing an essential role in plant tolerance to hypoxia (Perata and Alpi, 1993). While *pgm* and *ctr1* are well known to display reduced growth, *ein2.1* and *adh1* mutations do not have a major impact on growth, at least based on the original reports describing these mutants. The *ctr1* mutant constitutively displays phenotypes associated to ethylene signaling, whose consequences include extreme dwarfism (Kieber et al., 1993). The *ein2.1*, which is insensitive to ethylene, instead displays minor phenotypic differences when compared to the wild-type, although it has been reported to grow slightly bigger (Guzmán and Ecker, 1990). The *pgm* mutant is smaller than the wild-type (Caspar et al., 1985). Interestingly, the growth of a similar mutant (starch-free 1; *stf1*) was recently studied by digital imaging, providing an interesting benchmark for our study (Wiese et al., 2007). Further details on growth conditions are provided in Experimental Procedures.

Brief Overview of the Phenotiki System

Phenotiki is composed of an affordable image acquisition device (less than 200€ in material cost) and a suite of (standalone or web-based) software tools for image analysis. Phenotiki's architecture is illustrated in Figure 1.

The Phenotiki device consists of a Raspberry Pi embedded computer (The Raspberry Pi Foundation, Caldecote, UK, http://www.raspberrypi.org) operating the RaspiCam

fixed-focus (and fixed-zoom) imaging sensor. As Figure S1 shows, the device is small (10×6.5×3.5 cm) and lightweight (115 g) and it was affixed with zip ties to the growth chamber's ceiling. The device was enclosed in plastic housing (Figure S1) and could wirelessly connect to the Internet after it was setup (a complete equipment list is provided in Methods S1). We devised a graphical software (Figures 1b and S2, and Movie S1) for ease of interaction with the device, which permitted to define acquisition schedule and parameters for time-lapse 2D optical imaging of the scene and data transmission. Phenotiki was calibrated and configured to acquire top-view images (Figure 2a) with preset time schedule (every 12 hours, respectively, at the beginning and the end of the 12 hour photoperiod) and fixed imaging conditions (e.g., focus, exposure, field of view) over a period of 26 days, resulting in a time-lapse sequence of 52 images in total.

Data storage and processing were decoupled from acquisition. Image data can be transmitted over the local network or the Internet to a centralized repository (on site or remote) for analysis. Our device can also directly connect to CyVerse (formerly iPlant Collaborative, http://www.cyverse.org) to upload data and using our modules built upon the BisQue framework (Goff et al., 2011) can offer a cloud-based application to store and analyze the images for higher throughput potential (see Methods S2 for the naming of modules on CyVerse). For this paper, results were obtained based on the standalone software after imaging data were collected at a local workstation.

The same software base is used in both the standalone and the cloud applications (screenshots shown in Figures 1c-d, S3, and S4, and usage demonstrated in Movies S2 and S3). Robust (and validated) image processing algorithms have been efficiently implemented to enable annotation, detection, tracking and segmenting plants from background (Minervini et al., 2014), and also counting leaves automatically (Giuffrida et al., 2015). These are available as modules that can be either used through the standalone graphical interface (Figure S3) or in the web-based application (Figure S4). This design also demonstrates how our platform can be extended to address future hypotheses.

We obtained phenotypic information related to plant growth, morphology, color, and leaf count. Measurements were exported from our software in machine-readable format and were imported to MATLAB (The MathWorks, Inc., Natick, MA) and R (The R Foundation, Vienna, Austria) for visualization and statistical analysis. The plant segmentation and leaf counting components of our system can operate autonomously on large datasets once they have been configured. Before analyzing the entire dataset for plant growth, we annotated one image (i.e., delineating the plants from background, a task that can be completed efficiently with the aid of our semi-interactive annotation tool, described in detail in Methods S2 and S3), on the basis of which optimal operational parameters were found automatically by our software through an optimization process, thus eliminating the need for the user to trial parameters. The same parameters were applied to the entire image sequence of the experiments presented herein. We also used annotations of the number of plant leaves for a set of representative training images to learn a model that can estimate leaf count of unseen images and then applied this model to the entire dataset.

Software and sensor setup instructions are in the public domain at http://phenotiki.com. Further details on imaging setup, computer vision approaches, and the definition of the scored visual traits (see also Figure S5) are provided in Experimental Procedures and in Methods S2, S3, and S4. Measurement validation with non-image measurements and comparison with a higher-grade camera follow the presentation of phenotypic findings.

Phenotypic Results

Phenotyping Plant Area and Morphology

We compared rosette size achieved by different genotypes based on projected leaf area (PLA), diameter, and perimeter. Results are shown in Figure 3a, c, d. Separate repeated measures ANOVA with the Greenhouse-Geisser correction were used to assess effects on each of the descriptors, of time (within-subject factor), genotype (between-subject factor), and their interaction. For all three descriptors there was a significant time-genotype interaction ($P<0.01$). Tukey-Kramer multiple comparison ($P<0.05$)

revealed that three distinct groups can be identified: Col-0 and *ein2.1* presented the largest size; *adh1* and *pgm* presented medium size; *ctr1* exhibited extreme dwarfism and hence the smallest size. These results were expected for *pgm* (Apelt et al., 2015; Caspar et al., 1985) and *ctr1* (Kieber et al. 1993). In the case of *ein2.1* a larger plant diameter was previously reported for 24-days-old plants (Guzmán and Ecker, 1990) while our data showed a plant diameter slightly smaller than the wild-type in the case of *ein2.1* (Figure 3c). No obvious phenotypes were previously reported for *adh1* mutants. Since the enzyme ADH is involved in hypoxia tolerance it is tempting to speculate that the adopted watering plan (twice a week by sub-irrigation for all plants) might have led to root hypoxia for *adh1* mutants, which are more sensitive to watering level, with consequences on plant growth.

Compactness data did not suggest any evident groupings (Figure 3e). However, note that *ein2.1* presented higher compactness than Col-0 ($P<0.01$, paired t-test), although they shared similar size. Higher stockiness was consistently observed for *ctr1* with respect to the other genotypes (Figure 3f), although this may be partly due to considerably smaller size of the *ctr1* plants and fixed (per plant) imaging resolution, so that the extremely dwarf plants will appear concentrated and more circular.

We also adopted a parametric model-driven approach to growth analysis based on Richards' growth curve (Methods S5) and observed PLA data, the result of which is shown in Figure S6 and Table S1. Average normalized growth rates indicated slower growth for *ctr1* and *pgm* with respect to the other genotypes. In fact, the time of inflection in the growth curves (γ) of *ctr1* and *pgm* was estimated, respectively, at approximately 42 and 36 days after sowing, whereas for the wild-type at 30 days after sowing. Finally, based on 95% confidence intervals for estimated value of parameter k, we observed that the growth rate of *pgm* was significantly lower than Col-0, *ein2.1*, and *adh1*.

Phenotyping Growth Stage Based on Leaf Counting

We also compared leaf-counting progression (Figure 4a) and developmental growth stages among genotypes, which, based on the scale discussed in Boyes et al., 2001, are

identified by the number of leaves. In Figure 4b we highlight at which day after sowing a group of plants (i.e. genotype) developed 4 leaves (1.04), 10 leaves (1.10), 14 leaves (1.14), and later leaf-related stages (>1.14), respectively. In accordance with the previous analysis based on plant size, we observe that *ein2.1* and Col-0 reached successive growth stages more rapidly than the other genotypes, with *pgm* and *ctr1* producing new leaves at a markedly slower pace than the wild-type. A pairwise Tukey-Kramer comparison (following a significant repeated measures ANOVA) on leaf count data, as plotted in Figure 4a, confirmed that *adh1*, *pgm*, and *ctr1* differed from the wild-type ($P<0.05$, cf. Table S3).

Phenotyping Diel Growth Dynamics

Differences in diurnal and nocturnal growth rates were assessed based on average (aggregated throughout the experiment) relative growth rate (RGR), using one-way ANOVA followed by Tukey-Kramer multiple comparison amongst the five groups with results shown in Figure 5. Overall, considering a diel growth cycle, *ctr1* presented lower RGR than the other genotypes ($P<0.01$). Also *ein2.1* had lower growth rate than control ($P<0.05$). When considering diurnal growth, *pgm* exhibited considerably higher (approximately double) growth rate than the other genotypes ($P<0.01$). During night time, growth of *pgm* decreased considerably. Reduced nocturnal growth was previously reported by Wiese et al., 2007, using the *stf1* mutant, that, as in the case of *pgm*, is defective in the plastidial phosphoglucomutase enzyme. Differences in diurnal and nocturnal growth rate within genotype were assessed via paired t-test, which was significant for *pgm* and *ctr1* ($P<0.01$), showing preferential growth during the day, and also for *adh1* ($P<0.05$). On the other hand, no significant difference in diurnal and nocturnal RGR was observed for *ein2*.1 and Col-0. Daily cyclic patterns as evident in Figure 3 were also demonstrated by power spectral density estimation of the PLA data (of Figure 3a) shown in Results S1.

Phenotyping Color

Color appearance of plant subjects was in general bright green, and after an initial adjustment it did not vary significantly throughout the experiment (Figure 3b). On the

other hand, a comparison among groups revealed that color appearance of *adh1* was statistically different to the other genotypes. We measured color changes quantitatively using the HSV (Hue, Saturation, Value) color space. On average, color appearance of *adh1* (Hue=77°) differed from all the other genotypes (Hue=82°) with a drift towards yellow hues (Figure 3b), as highlighted by a repeated measures ANOVA followed by Tukey-Kramer multiple comparison (P<0.01). The yellowish color of *adh1* again suggests that the plants suffered from root hypoxia and this trait was found by our analysis based on Phenotiki.

Measurement Validation

Validating Plant Growth Measurements

Central to measuring plant growth in our software is the algorithm for delineating (segmenting) the plants from background. While previously the plant segmentation algorithm has been validated against manual image-based plant delineations showing 97% overlap agreement (Minervini et al., 2014), here we compare its performance to the traditional non-image based measurement approach, as done by others (De Vylder et al., 2012). Specifically, we recorded the diameter of each subject measured on a daily basis at the end of the photoperiod using a digital caliper, obtaining overall 360 manual measurements. Those were compared with image-based calibrated values obtained automatically using our software on the corresponding images. The scatter plot in Figure 6a shows excellent agreement between automatic and manual measurements, with a concordance correlation coefficient for repeated measures $\rho_{CCC,RM}$=0.997 (lower 95% confidence limit = 0.995), which is proper for longitudinal studies when within-subject correlation may exist due to repeated measures (Carrasco et al., 2013). Additionally, the quantile-quantile plot in Figure 6b shows that measurements obtained with the two methods follow similar distributions. To demonstrate that our accuracy is consistent across measurement range, the Bland-Altman (B-A) plot in Figure S7 compares measurement difference with the mean for each pair of observations. The B-A analysis was conducted with the method by Bland and Altman, 2007, that accounts for repeated measures. The average measurement was 3.655 cm and given the small bias

-0.048 cm and 95% limits of agreement (mean difference±1.96SD) from -0.394 to 0.298 cm, we can conclude that automatic and manual measurements of rosette diameter were in excellent agreement.

Comparison with a Higher Grade Camera with Optical Zoom

The Phenotiki device utilizes the *RaspiCam* fixed-focus camera to acquire images of the scene. Due to the absence of moving parts and focusing options, cameras with fixed focus are cheaper and easier to set than those with autofocus or manual focus, however, the latter in general provide higher-quality images. To assess whether such higher quality provides any additional benefits (e.g., higher statistical power) to a similar phenotyping experiment as ours, we used also a more expensive consumer grade *Canon* camera with movable optics, that has a higher effective resolution due to the movable lens (zoom), but also because it was placed to image at an effective field of view assuming imaging at 50 cm (typical of a growth shelf). To permit the comparison, the Canon was installed alongside the RaspiCam, to take images of the same plants and arrangement at exactly the same time of the day.

First, we validated the Canon sensor against manual measurements of rosette diameter. Repeating the same regression and Bland-Altman type analyses, as described previously, no differences were found in measurement accuracy with manual measurements (Figure S8). Comparing limits of agreement and bias between Canon and RaspiCam, differences were minimal (Figures S7 and S8) indicating that with respect to manual measurements there was no difference between the two camera sensors.

We repeated all the phenotypic analyses described in the previous section using images from the Canon camera. In all cases we observed agreement on the statistical differences already found using the RaspiCam. As an example, Table S2 compares the results of the pairwise Tukey-Kramer comparison (following a significant repeated measures ANOVA) between PLA data of different genotypes obtained respectively with RaspiCam and Canon sensor. Observe that *P*-values are close to each other and at the 0.05 significance level conclusions are the same.

Finally, to determine if sensor quality was a factor we pooled PLA data measured respectively by RaspiCam and Canon, and added camera type as an additional factor to the above ANOVA setting. We found that camera type was insignificant (P=0.696).

Validating Leaf Counting

To automatically estimate the number of plant leaves in 2D images without 3D information, we devised a machine vision algorithm that predicts the number of leaves based on plant features in the images that are learned in a data-driven fashion (Giuffrida et al., 2015).[1] For the purpose of this validation experiment, all image data were labeled by a human expert (with the use of the annotation tool) to associate the number of leaves to each of the 1248 plant images in our dataset, that were used to train and evaluate the method.

Figure 4 shows the time series of the number of leaves for each genotype (Figure 4c) and growth progression bar (Figure 4d) as derived from the expert annotations. One can readily observe that growth trends are in agreement between predicted and ground-truth counts (Figure 4a, c). This is also evident when visualized with growth progression bars (Boyes et al., 2001) of the predicted (Figure 4b) and expert derived data (Figure 4d), demonstrating that our algorithm can detect specific growth stages of a plant (Principal Growth Stage 1, Boyes et al., 2001).

Quantitative analysis is shown in Table 1, reporting four (now standard) evaluation metrics (Scharr et al., 2016), which compare agreement between ground-truth and predicted count as: difference in count (DiC), absolute difference in count ($|DiC|$), mean squared error (MSE), and coefficient of determination (R^2). With respect to the algorithm presented in Giuffrida et al., 2015, Phenotiki adopts an extended version that relies on image features and also plant genotype and projected leaf area variables to estimate the number of leaves (further details can be found in Experimental Procedures). The results produced by the algorithm agree with leaf counts made by expert inspectors (R^2=0.94 on the testing set), with mean and standard deviation less

[1]An earlier version of this algorithm won the first place in the 2015 edition of the Leaf Counting Challenge (http://www.plant-phenotyping.org/CVPPP2015-challenge).

than 1 in absolute count ($|DiC|$). Automated leaf counts differed from an expert's manual count by not more than one leaf in 83% of examples.

As a further validation, we evaluated if interchanging the expert data with the automated predictions had any effect in statistical comparison testing. Table S3 compares the results of the pairwise Tukey-Kramer comparison (following a significant repeated measures ANOVA) between count data of different genotypes obtained respectively with the expert data and automated counting. Observe that *P*-values are close to each other and at the 0.05 significance level phenotypic conclusions are the same.

DISCUSSION

We presented an affordable and easy to use solution to plant phenotyping. It was validated using a proof-of-concept phenotyping experiment with Arabidopsis genotypes (some of which with known growth characteristics) to demonstrate that, despite the employment of low-cost hardware, it can characterize growth in a satisfactory fashion. The system was validated extensively using non-image based methods via measuring rosette diameter with a caliper and also using expert annotation of the images via manual counting of plant leaves. The underlying plant segmentation algorithm has also been previously validated with manual delineations of plants (Minervini et al., 2014). Furthermore, it was also compared with a higher-grade camera that had movable optics. Overall, we found no significant differences between the measurements obtained with our system and those obtained with other means.

We adopted a distributed design and decoupled sensing from analysis and storage. This lowered the cost of the device and provides scalability. We rely on an off-the-shelf embedded computer (the Raspberry Pi) and a fixed-optics camera sensor for several reasons. The Raspberry Pi is affordable and offers sufficient computational power; furthermore, it has a large following and a vast user and development community, and several core suppliers. This credit-card sized yet complete computer attached to the imaging sensor can be used for storage (i.e., the device can serve even as simple data logger), but is used in Phenotiki to control the imaging sensor and transmit data to the

computational unit. The fixed optics sensor offers robustness to environmental conditions by reducing condensation effects due to lack of movable parts –alternatively, moving optics cameras require expensive housing to protect against condensation.

Our device can be setup in less than one day. Hardware components can be easily obtained from one of the many suppliers. Additional step-by-step instructions on assembling and installing the device and software are available on the Phenotiki website (http://phenotiki.com).[2] This also installs the software that allows the control and setup of the imaging settings via web-based interface. In addition, it provides guidelines to calibration processes. The device can be attached to growth chambers or shelves and requires a single cable for power. Once installed it can operate unattended with the same imaging parameters and requires virtually no maintenance when not displaced. This level of technology readiness is unprecedented for an affordable, yet integrated, plant phenotyping setting.

Due to its small footprint, the device easily fits in a growth chamber and does not cover much of the chamber lights. For example, by installing it 1 m above the plants, the camera ensures a field of view of 0.5 m^2, which would permit the imaging of about 60 Arabidopsis plants grown in pots throughout their life cycle, with an imaging resolution suitable for the phenotyping applications shown in this article. Equivalently, when placed 50 cm above the plants, the device can image approximately 30 subjects offering even higher resolution. Informal discussions with several plant scientists confirmed that this is adequate when pilot studies are sought-after. The system can reach higher throughput while still maintaining affordability by increasing the number of sensors: due to its compact size and low cost, multiple Phenotiki devices can be readily deployed to offer even higher imaging resolution or throughput. Thus, we avoid complex and costly solutions based on robotics and actuation (as for example in Tisné et al., 2013) that typically have larger footprint reducing further the already hard to find growth chamber space, and require specific know-how and maintenance, necessitating

[2] We maintain software and user manuals at an external repository to permit their continuous updating.

additional in-house expertise (which may not be available at length) or service contracts (when development has been outsourced).

The imaging data acquired by the device are sent to a local workstation or to the cloud. The on-site data hosting and processing on a workstation is ideal for laboratories with expected small throughput and for users who prefer to rely on local, in-house computational infrastructure. On the other hand, our distributed approach permits to outsource storage and computation to the cloud, thus relieving the user from the cost of purchasing and maintaining a high-performance computing infrastructure in situ when throughput will be high. Furthermore, by relying on the cloud, the additional computational needs to analyze higher throughput data can be readily met due to its immediate resource scalability, and the implementation of asynchronous upload mechanisms that are used by our device to send data to the cloud. When the available network bandwidth (could occur in laboratories in countries with poorer Internet infrastructure) or storage capacity are limited we can potentially integrate image compression algorithms within the Phenotiki device (Minervini and Tsaftaris, 2013; Minervini et al., 2015c).

Our analysis software and graphical interface are built on top of MATLAB and are publicly available to the academic community. We provide pre-compiled versions of the software that do not require a MATLAB installation or license and can be executed standalone. Our source code is also available to permit third-party extensions. For those that do not want to rely on local processing, image analysis modules of Phenotiki for plant segmentation and annotation are available on the BisQue platform provided by CyVerse (Goff et al., 2011). Our interface is intuitive and our software is designed in a modular fashion, such that new analysis pipelines can be integrated.

Most of the available software for plant phenotyping (http://plant-image-analysis.org, Lobet et al., 2013) are tuned to specific setups and assumptions. Instead, we wanted to create software that can be potentially adopted in a variety of experimental settings with minimal adaptation (e.g., finding suitable parameters or annotating training data), anticipating that it will be used by several laboratories. This necessitates image processing algorithms that can adapt. Approaches that rely on constraining the

experimental setting and applying thresholds on image intensity values (e.g., De Vylder et al., 2012; Easlon and Bloom, 2014) are not readily portable across different labs because they offer limited robustness to varying conditions (e.g., changes in plant appearance due to senescence or treatment), changes in illumination (e.g., different daylight conditions), or unplanned alterations in the background (e.g., algae growing on soil). In fact, the need for robust image analysis algorithms and software has been labeled as the new bottleneck in plant phenotyping (Minervini et al., 2015b; Tsaftaris et al., 2016).

Our software can reliably extract plant growth traits, color traits, and leaf count based on efficient implementations of validated algorithms centered in state-of-the-art methods of image processing and machine learning (Giuffrida et al., 2015; Minervini et al., 2014; Minervini et al., 2015a), which are designed to provide robustness to variable experimental settings and perform well with 2D fixed-focus imaging. Although leaf count has been used also previously as a phenotypic parameter (Arvidsson et al., 2011; Jansen et al., 2009), here we adopt a learning-based object counting method for plant leaves using affordable 2D-based vision without the need for expensive (and low throughput without actuation) 3D vision (Apelt et al., 2015).

To provide a reference of the computational time required by our image analysis software, on a local workstation (Intel Xeon CPU 3.50 GHz, 64 GB RAM, and running Linux), plant segmentation and morphological traits extraction took about 5.5 seconds per tray image (24 plants). Training the leaf counting model on a dataset composed of 200 single plant images required ~3.5 minutes. Predicting the number of leaves of a plant using the learned model took less than a second per plant image.

Central to our software design and machine learning is the notion of training (annotated) data to learn from. We use them to learn how to count leaves for a specific plant species, and also to optimize parameters to make the algorithms adapt to new experimental settings, relieving the user from manually tuning parameters. To help alleviate the process of creating annotated data we also provide an interactive tool for plant and leaf level annotations that uses state-of-the-art image processing techniques to minimize expert input (Minervini et al., 2015a). We observed that annotating plant

leaves using our tool (a byproduct of which are also leaf count and plant segmentation) requires on average less than 3 minutes, in contrast with a completely manual approach requiring on average 30 minutes for a trained operator to annotate a single plant. Annotating only for the purpose of leaf counting (which involves clicking on each leaf, to help mental memory) takes ~1 minute per plant.

Phenotiki has been primarily tested on Arabidopsis. However, due to its open architecture and choice of algorithm design, we envision that with suitable choices of algorithm parameters[3] the Phenotiki platform could be used to image and extract traits also in other plant species. To provide guidance we discuss briefly this potential. The plant segmentation algorithm and the leaf annotation tool are agnostic to plant shape and could potentially be used for plants with different structure than Arabidopsis. In fact, the annotation tool was evaluated also on publicly available tobacco plant data (Minervini et al., 2015a). The leaf counting method in its current form relies on the radial arrangement of leaves to learn the model, so it could potentially be used for other plants with radial arrangement of leaves (as evidence from an open challenge on publicly available data suggest (Giuffrida et al., 2015)). Overall we anticipate that our methods can be used also with different imaging settings (e.g., different scene background, different field of view, and others), as long as adequate feature resolution is present.

Currently, we do not have available a fully-automated leaf segmentation algorithm, which might be necessary for investigations into differential leaf growth. However, a suitable surrogate could be obtained with counting as performed in this article, which could be used to assess plant status and leaf emergence (Apelt et al., 2015). On the other hand, the interactive annotation tool can be used also for semi-automated leaf segmentation, and we are working towards propagating information to subsequent images in the time-lapse to reduce user interaction. More encouraging are the findings of a recent collation study and more recent papers using open access data (Minervini et al., 2016) on automated leaf segmentation (Scharr et al., 2016; Pape and Klukas, 2015) and other studies (Tessmer et al., 2013; Yin et al., 2014) which in the future could be

[3] We offer a grid search module that helps to find a suitable set of parameters using some annotated data.

integrated in our platform. Results reported show a promising average of 70% accuracy in leaf segmentation on the basis of single 2D images.

We envision the emergence of a community that supports and fosters the continued development of the system, and thanks to the modular design of our framework user contributions will evolve the device and software to match the needs of diverse and specialized applications. As an example, we mention the efforts of McCormick and colleagues (University of Edinburgh, UK), who inspired by an earlier prototype of the Phenotiki device, have introduced a near infrared imaging sensor permitting also night-time imaging of rosette plants (manuscript in preparation). To further facilitate development, parts of our data and expert annotations are available openly (Minervini et al., 2016) and have already been used by the broad image analysis community (Pape and Klukas, 2015; Romera-Paredes and Torr, 2016; Scharr et al., 2016).

In conclusion, Phenotiki offers a complete hardware and software solution to affordable phenotyping offering an out-of-box experience. By relying on open software and open hardware we hope to lower the entry barrier and promote adoption of image-based phenotyping technologies.

EXPERIMENTAL PROCEDURES

Plants and Growth Conditions

The experimental setup included the following Arabidopsis lines (NASC accession as NX...X): ecotype Col-0 (5 subjects), *pgm* (plastidial phosphoglucomutase, N210; 5 subjects), *ctr1* (constitutive triple response 1, N8057; 5 subjects), *ein2.1* (ethylene insensitive 2.1, N65994; 5 subjects), *adh1* (alcohol dehydrogenase 1, N552699; 4 subjects). Plants were grown in individual pots under 12-hour light/12-hour dark regime; artificial daylight illumination was provided by cool-white fluorescent lamps (~100 μmol photons m^{-2} s^{-1} light intensity). Temperature was on average ~22°C [daytime] and ~16°C [night-time]. Watering was provided twice a week by sub-irrigation. Pots were spaced out in the tray to prevent adult plants from touching.

Arrangement of genotypes in the tray was randomized to eliminate possible bias in the results due to variations in watering or lighting conditions (Figure 2b). No treatments were performed.

The Phenotiki Device

Our affordable and compact device (Figures 1a and S1) is based on the Raspberry Pi single-board computer (The Raspberry Pi Foundation, http://www.raspberrypi.org) used to control an OmniVision OV5647 fixed-optics CMOS camera sensor (known as *RaspiCam*), with the ability to capture 5 megapixel static images of the scene (Figure 2a) in the visible spectrum (i.e., RGB color images). A complete list of the equipment used to setup the Phenotiki device and corresponding operating specifications are provided in Methods S1. While we used the Raspberry Pi 1 model B, more recent versions with higher computational power are also available at the same cost. In addition, the new RaspiCam V2 version offers higher resolution (8 megapixels). Other types of sensors (e.g., a higher grade camera or environmental monitoring sensors) can be directly attached to the Raspberry Pi via USB (Universal Serial Bus) or GPIO (General Purpose Input/Output). To facilitate configuration and monitoring of the device, we deployed a web-based graphical user interface to operate it remotely from a laptop or a smartphone (Figures 1b and S2, Movie S1). To reduce storage requirements without affecting phenotyping accuracy (Minervini et al., 2015c), images were encoded at the device using the lossless compression standard available in the PNG file format (although Phenotiki supports a variety of lossless and lossy image formats). At the end of the experiment, a ZIP archive containing all the acquired images was automatically created on the Phenotiki device, and via the web-based interface of the device we downloaded it to a local workstation for archival and processing (Figure S2). Phenotiki can also directly upload data to CyVerse (with additional options such as upload to FTP servers or cloud storage services in development).

Imaging Configuration and Setup

The Phenotiki device was placed approximately 1 m above the plants, affixed via zip-ties on the framework of our chamber. On the basis of a calibration scale we measured an effective pixel resolution of 0.323 mm. At this distance a maximum of 60 Arabidopsis plants grown in pots can be imaged (or up to 80 Arabidopsis rosettes in juvenile stages of development). To obtain consistent color information, a white reference card was included to perform automatic white balancing upon image acquisition.

In addition, another higher grade camera (Canon PowerShot SD1000, shorthanded as *Canon*) was also used that had movable optics and could adjust field of view via optical zoom. This sensor was set to image at an effective distance of 50 cm which is common in growth chambers. This effective distance dictated also the number (24) of subjects used in this study. The diameter of each plant was manually measured with a caliper and recorded on a daily basis for reference.

Image Analysis Protocol

The acquired imaging data were processed using our image analysis software, which has been designed to operate on images showing a top view on rosette-shaped plants and relies on the algorithm by Minervini et al., 2014. To isolate plant from background –a process known as segmentation– the algorithm first localizes automatically plant objects in the tray by placing a bounding box around each plant, then each plant is segmented from background. To enable association across time, plants from consecutive images are matched (i.e., tracked). Segmenting plants in images acquired in a general laboratory setting can be a challenging task under typical growth chamber conditions (e.g., green algae growing on the soil surface, water reflections, light inhomogeneity, changes in color and appearance of the plants due to senescence or treatments). Therefore, the adopted algorithm relies on machine learning and a probabilistic (prior-driven) level set-based active contour model for accurate plant segmentation that can adapt to scene variability (Minervini et al., 2014). Since the

algorithm requires the tuning of several parameters to achieve this adaptation, we provided via a semi-automated tool a pre-annotated tray image upon which the algorithm automatically finds optimal parameters (see Methods S2). We applied the algorithm and found parameters on the images of the experiment and we extracted a variety of traits to describe rosette size (area, diameter, perimeter), morphology (compactness, stockiness), growth stage progression (leaf count), and color, obtaining for each plant a multivariate temporal description of its visual phenotype. For leaf count, we extended a state-of-the-art method that predicts automatically the number of visible rosette leaves (Giuffrida et al., 2015). This learning-based approach requires a set of annotated training images of single isolated plants and corresponding integer number of visible leaves (i.e., the actual per-image leaf count). Given a set of training images, the algorithm learns the features (templates composed of square patches) and a regression model to predict the number of leaves. Since the original algorithm by Giuffrida et al., 2015, was designed to be agnostic to scale (in order to accommodate by design the variable distance between sensor and camera of the images in the challenge dataset, see further explanation in Table S4) and was tested on a challenge dataset that did not provide genotype information, we added two extra features: plant genotype (categorical variable) and projected leaf area (PLA, continuous variable). These properties provide to the algorithm information related to the typical temporal growth behavior, or more generally speaking the dose-response characteristics of each plant (Poorter et al., 2013). The categorical genotype variable was encoded as five separate dummy variables. Note that the method does not per-se use the actual genotype information (e.g., does not know that the first dummy is Col-0). The new features vector is then standardized by subtracting the mean and dividing by the standard deviation. (Further parameter settings are shown in Table S4.)

To facilitate adoption, our image analysis solution is publicly available as a standalone MATLAB-based tool (albeit no MATLAB installation or license is required) and is accompanied by an easy-to-use and intuitive graphical user interface (Figures 1c and S3, and Movie S2) and also as a web application running on the CyVerse cloud (Figures 1d and S4, and Movie S3). The software offers the possibility to analyze image datasets

and export or visualize phenotypic results. Additionally, annotation tools are available for the user to provide feedback or labeled data (e.g., segmented plants or number of leaves) which are used to train the models of the learning components in the image analysis pipeline. All code is open source.

The Phenotiki software was designed in a modular fashion. In the standalone version, the user is presented with an integrated view in which several modules are available to address a variety of tasks. The modules communicate via a shared data structure (Figure S9) encapsulating all the metadata associated with an experiment (e.g., subjects, genotypes, acquisition time, user annotations), and populated or augmented with analysis results (e.g., plant segmentation masks, phenotype descriptors) obtained after a module execution. The cloud-based version of the Phenotiki software follows a similar design, with the modules integrated in a composite application within the BisQue framework (Goff et al., 2011).

ACKNOWLEDGMENTS

This work was partially supported by a Marie Curie Action: "Reintegration Grant" (256534) of the EU's FP7. We thank Nirav Merchant for providing us access to the CyVerse platform and the support of Kristian Kvilekval and Dmitry Fedorov for helping us to integrate our software within BisQue. We acknowledge the help of Fabiana Zollo in the implementation on BisQue. Finally, we thank Hanno Scharr, Alistair McCormick, and Antonio Masi for providing feedback on the manuscript. The authors declare no conflicts of interest.

SUPPORTING INFORMATION

Figure S1. Pictures of the proposed affordable Phenotiki device.

Figure S2. Screen captures of our web-based software tool to configure and operate the Phenotiki device.

Figure S3. Screen captures showing the user interface of our standalone plant image analysis software.

Figure S4. Screen captures of our suite of web-based applications for plant image analysis on the CyVerse cloud platform.

Figure S5. Illustration of some of the visual traits extracted by our system.

Figure S6. Richards' growth curve fitted to PLA data of each genotype.

Figure S7. Bland-Altman plot showing the agreement between rosette diameter measured with Phenotiki and manually with a caliper.

Figure S8. Agreement between rosette diameter measured automatically from images acquired with a Canon camera and manually with a caliper.

Figure S9. Data structure adopted in the Phenotiki analysis software.

Table S1. Parameter estimates of the Richards' growth curve fitted to PLA data.

Table S2. Pairwise comparisons of PLA results between Col-0 and the other genotypes.

Table S3. Pairwise comparisons of leaf count results between Col-0 and the other genotypes.

Table S4. Parameters setting of the automatic leaf counting algorithm.

Methods S1. List of hardware equipment used to setup the Phenotiki device.

Methods S2. Additional description of the Phenotiki image analysis software.

Methods S3. Overview of the computer vision approaches adopted in the Phenotiki image analysis software.

Methods S4. Plant visual trait descriptors extracted by Phenotiki.

Methods S5. Parametric growth analysis based on Richards' curve.

Results S1. Power spectral density estimation of the PLA data highlighting daily cyclic growth patterns.

Movie S1. Demo of the web-based software to configure the Phenotiki device.

Movie S2. Demo of the standalone Phenotiki image analysis software.

Movie S3. Demo of the Phenotiki image analysis modules on BisQue/CyVerse.

REFERENCES

Apelt, F., Breuer, D., Nikoloski, Z., Stitt, M. and Kragler, F. (2015) Phytotyping 4D: A light-field imaging system for non-invasive and accurate monitoring of spatio-temporal plant growth. *The Plant Journal*, 82, 693–706.

Arvidsson, S., Pérez-Rodríguez, P. and Mueller-Roeber, B. (2011) A growth phenotyping pipeline for Arabidopsis thaliana integrating image analysis and rosette area modeling for robust quantification of genotype effects. *New Phytologist*, 191, 895–907.

Bland, J.M. and Altman, D.G. (2007) Agreement between methods of measurement with multiple observations per individual. *Journal of Biopharmaceutical Statistics*, 17, 571–582.

Bours, R., Muthuraman, M., Bouwmeester, H. and van der Krol, A. (2012) OSCILLATOR: A system for analysis of diurnal leaf growth using infrared photography combined with wavelet transformation. *Plant Methods*, 8, 1−12.

Boyes, D.C., Zayed, A.M., Ascenzi, R., McCaskill, A.J., Hoffman, N.E., Davis, K.R. and Görlach, J. (2001) Growth stage-based phenotypic analysis of Arabidopsis. *The Plant Cell*, 13, 1499−1510.

Brown, T.B., Cheng, R., Sirault, X.R.R., Rungrat, T., Murray, K.D., Trtilek, M., Furbank, R.T., Badger, M., Pogson, B.J. and Borevitz, J.O. (2014) TraitCapture: Genomic and environment modelling of plant phenomic data. *Current Opinion in Plant Biology*, 18, 73–79.

Carrasco, J.L., Phillips, B.R., Puig-Martinez, J., King, T.S. and Chinchilli, V.M. (2013) Estimation of the concordance correlation coefficient for repeated measures using SAS and R. *Computer Methods and Programs in Biomedicine*, 109, 293–304.

Caspar, T., Huber, S.C. and Somerville, C. (1985) Alterations in growth, photosynthesis and respiration in a starchless mutant of Arabidopsis thaliana (L.) Heynh deficient in chloroplast phosphoglucomutase activity. *Plant Physiology*, 79, 11−17.

De Vylder, J., Vandenbussche, F., Hu, Y., Philips, W. and Van Der Straeten, D. (2012) Rosette Tracker: An open source image analysis tool for automatic quantification of genotype effects. *Plant Physiology*, 160, 1149−1159.

Easlon, H.M. and Bloom, A.J. (2014) Easy Leaf Area: Automated digital image analysis for rapid and accurate measurement of leaf area. *Applications in Plant Sciences*, 2, 1–4.

Furbank, R.T. and Tester, M. (2011) Phenomics – Technologies to relieve the phenotyping bottleneck. *Trends in Plant Science*, 16, 635−44.

Goff, S.A., Vaughn, M., McKay, S., Lyons, E., Stapleton, A.E., Gessler, D., Matasci, N., Wang, L., Hanlon, M., Lenards, A., Muir, A., Merchant, N., Lowry, S., Mock, S., Helmke, M., Kubach, A., Narro, M., Hopkins, N., Micklos, D., Hilgert, U., Gonzales, M., Jordan, C., Skidmore, E., Dooley, R., Cazes, J., McLay, R., Lu, Z., Pasternak, S., Koesterke, L., Piel, W.H., Grene, R., Noutsos, C., Gendler, K., Feng, X., Tang, C., Lent, M., Kim, S., Kvilekval, K., Manjunath, B.S., Tannen, V., Stamatakis, A., Sanderson, M., Welch, S.M., Cranston, K., Soltis, P., Soltis, D., O'Meara, B., Ane, C., Brutnell, T., Kleibenstein, D.J., White, J.W., Leebens-Mack, J., Donoghue, M.J., Spalding, E.P., Vision, T.J., Myers, C.R., Lowenthal, D., Enquist, B.J., Boyle, B., Akoglu, A., Andrews, G., Ram, S., Ware, D., Stein, L. and Stanzione, D. (2011) The iPlant Collaborative: Cyberinfrastructure for plant biology. *Frontiers in Plant Science*, 2, 1−16.

Giuffrida, M.V., Minervini, M. and Tsaftaris, S.A. (2015) Learning to count leaves in rosette plants. In *Proceedings of the Computer Vision Problems in Plant Phenotyping (CVPPP) Workshop*. BMVA Press, pp. 1.1–1.13.

Granier, C., Aguirrezabal, L., Chenu, K., Cookson, S.J., Dauzat, M., Hamard, P., Thioux, J.J., Rolland, G., Bouchier-Combaud, S., Lebaudy, A., Muller, B., Simonneau, T. and Tardieu, F. (2006) PHENOPSIS, an automated platform for reproducible phenotyping of plant responses to soil water deficit in Arabidopsis thaliana permitted the identification of an accession with low sensitivity to soil water deficit. *New Phytologist*, 169, 623–635.

Green, J.M., Appel, H., Rehrig, E.M., Harnsomburana, J., Chang, J.F., Balint-Kurti, P. and Shyu, C.R. (2012) PhenoPhyte: A flexible affordable method to quantify 2D phenotypes from imagery. *Plant Methods*, 8, 1–12.

Guzmán, P. and Ecker, J.R. (1990) Exploiting the triple response of Arabidopsis to identify ethylene-related mutants. *Plant Cell*, 2, 513–523.

Jansen, M., Gilmer, F., Biskup, B., Nagel, K.A., Rascher, U., Fischbach, A., Briem, S., Dreissen, G., Tittmann, S., Braun, S., De Jaeger, I., Metzlaff, M., Schurr, U., Scharr, H. and Walter, A. (2009) Simultaneous phenotyping of leaf growth and chlorophyll fluorescence via GROWSCREEN FLUORO allows detection of stress tolerance in Arabidopsis thaliana and other rosette plants. *Functional Plant Biology*, 36, 902–914.

Kieber, J.J., Rothenberg, M., Roman, G., Feldmann, K.A. and Ecker, J.R. (1993) CTR1, a negative regulator of the ethylene response pathway in Arabidopsis, encodes a member of the Raf family of protein kinases. *Cell*, 72, 427−441.

Leister, D., Varotto, C., Pesaresi, P., Niwergall, A. and Salamini, F. (1999) Large-scale evaluation of plant growth in Arabidopsis thaliana by non-invasive image analysis. *Plant Physiology and Biochemistry*, 37, 671−678.

Lobet, G., Draye, X. and Périlleux, C. (2013) An online database for plant image analysis software tools. *Plant Methods*, 9, 1−8.

Minervini, M., Abdelsamea, M.M. and Tsaftaris, S.A. (2014) Image-based plant phenotyping with incremental learning and active contours. *Ecological Informatics*, 23, 35−48.

Minervini, M., Fischbach, A., Scharr, H. and Tsaftaris, S.A. (2016) Finely-grained annotated datasets for image-based plant phenotyping. *Pattern Recognition Letters*, 81, 80–89.

Minervini, M., Giuffrida, M.V. and Tsaftaris, S.A. (2015a) An interactive tool for semi-automated leaf annotation. In *Proceedings of the Computer Vision Problems in Plant Phenotyping (CVPPP) Workshop*. BMVA Press, pp. 6.1–6.13.

Minervini, M., Scharr, H. and Tsaftaris, S.A. (2015b) Image analysis: the new bottleneck in plant phenotyping. *IEEE Signal Processing Magazine*, 32, 126–131.

Minervini, M., Scharr, H. and Tsaftaris, S.A. (2015c) The significance of image compression in plant phenotyping applications. *Functional Plant Biology*, 42, 971–988.

Minervini, M. and Tsaftaris, S.A. (2013) Application-aware image compression for low cost and distributed plant phenotyping. In *International Conference on Digital Signal Processing (DSP)*. IEEE, pp. 1–6.

Pape, J.M. and Klukas, C. (2015) Utilizing machine learning approaches to improve the prediction of leaf counts and individual leaf segmentation of rosette plant images. In *Proceedings of the Computer Vision Problems in Plant Phenotyping (CVPPP) Workshop*. BMVA Press, pp. 3.1−3.12.

Perata, P. and Alpi, A. (1993) Plant responses to anaerobiosis. *Plant Science*, 93, 1–17.

Poorter, H., Anten, N.P.R, and Marcelis, L.F.M. (2013) Physiological mechanisms in plant growth models: do we need a supra-cellular systems biology approach? *Plant, Cell and Environment*, 36, 1673–1690.

Romera-Paredes, B. and Torr, P.H.S. (2016) Recurrent instance segmentation. In *European Conference on Computer Vision (ECCV)*. Springer, pp. 312–329.

Rousseau, D., Dee, H. and Pridmore, T. (2015) Imaging methods for phenotyping of plant traits. In *Phenomics in Crop Plants: Trends, Options and Limitations*. Springer, pp. 61–74.

Scharr, H., Minervini, M., French, A.P., Klukas, C., Kramer, D.M., Liu, X., Luengo, I., Pape, J.M., Polder, G., Vukadinovic, D., Yin, X. and Tsaftaris, S.A. (2016) Leaf segmentation in plant phenotyping: a collation study. *Machine Vision and Applications*, 27, 585–606.

Sozzani, R., Busch, W., Spalding, E.P. and Benfey, P.N. (2014) Advanced imaging techniques for the study of plant growth and development. *Trends in Plant Science*, 19, 304–310.

Tessmer, O.L., Jiao, Y., Cruz, J.A., Kramer, D.M. and Chen, J. (2013) Functional approach to high-throughput plant growth analysis. *BMC Systems Biology*, 7, S17.

Tisné, S., Serrand, Y., Bach, L., Gilbault, E., Ben Ameur, R., Balasse, H., Voisin, R., Bouchez, D., Durand-Tardif, M., Guerche, P., Chareyron, G., Da Rugna, J., Camilleri, C. and Loudet, O. (2013) Phenoscope: An automated large-scale phenotyping platform offering high spatial homogeneity. *The Plant Journal*, 74, 534–544.

Tsaftaris, S.A. and Noutsos, C. (2009) Plant phenotyping with low cost digital cameras and image analytics. In *Information Technologies in Environmental Engineering*. Springer, pp. 238–251.

Tsaftaris, S.A., Minervini, M. and Scharr, H. (2016) Machine learning for plant phenotyping needs image processing. *Trends in Plant Science*, 21, 989–991.

Walter, A., Scharr, H., Gilmer, F., Zierer, R., Nagel, K.A., Ernst, M., Wiese, A., Virnich, O., Christ, M.M., Uhlig, B., Jünger, S. and Schurr, U. (2007) Dynamics of seedling growth acclimation towards altered light conditions can be quantified via GROWSCREEN: a setup and procedure designed for rapid optical phenotyping of different plant species. *New Phytologist*, 174, 447–455.

Wiese, A., Christ, M.M., Virnich, O., Schurr, U. and Walter, A. (2007) Spatio‐temporal leaf growth patterns of Arabidopsis thaliana and evidence for sugar control of the diel leaf growth cycle. *New Phytologist*, 174, 752–761.

Yin, X., Liu, X., Chen, J. and Kramer, D.M. (2014) Multi-leaf tracking from fluorescence plant videos. In *International Conference on Image Processing (ICIP)*. IEEE, pp. 408–412.

FIGURE LEGENDS

Figure 1. Overview of the Phenotiki system and screen captures showing the graphical user interfaces to operate its hardware and software components. (a) Schematic of the proposed distributed sensing and analysis framework illustrating the main components of our phenotyping platform. (b) Web interface to configure and operate the Phenotiki device from the browser. (c) Standalone version of the image analysis software. (d) Cloud-based version of the image analysis software that runs on a web browser.

Figure 2. Example imaging data acquired by the Phenotiki system. (a) Original image and (b) illustration of the randomized arrangement of the genotypes in the scene. (c) A growing *adh1* subject at different stages (numbers in red denote days after sowing), with the plant delineated via automatic segmentation (Minervini et al., 2014).

Figure 3. Plant size, morphology, and color (hue) traits (y-axis) plotted against time (x-axis). Measurements were taken for 25 days every 12 hours. Genotypes are identified by color and variance is denoted by shaded areas. The legend in panel (a) applies to all panels. To improve clarity of visualization of panel (b), a third-order Savitzky-Golay smoothing filter with kernel size of 7 was applied to each time series. Shown is also the HSV color wheel, with hue (H) values ranging from 0 to 360° and indication of the average value for *adh1* (77°) and for the other four genotypes collectively (82°).

Figure 4. Leaf counting data (a, b) estimated by our automated leaf counting algorithm and (c, d) derived from the expert annotations. Results are shown as (a, c) time series plots and (b, d) growth progression bars (Boyes et al., 2001). The learning-based counting algorithm was trained on a subset of plant images and then applied to the entire dataset.

Figure 5. Average RGR by genotype across the duration of the study (from 12 to 37 days after sowing). Shown are, respectively, diel, diurnal, and nocturnal RGR. Data are represented as mean ± standard error of the mean. The lines and asterisks above the bars indicate statistically significant differences in average RGR between genotypes as determined by Tukey-Kramer multiple comparisons test (* $P < 0.05$, ** $P < 0.01$).

Figure 6. Agreement between rosette diameter measured from images using Phenotiki (Automatic) and manually with a caliper (Manual). (a) Scatterplot with fitted linear regression (dashed red line) and 45° rising line (black solid line). (b) Q-Q plot with superimposed a red line joining the first and third quartiles of each distribution.

Figure 1

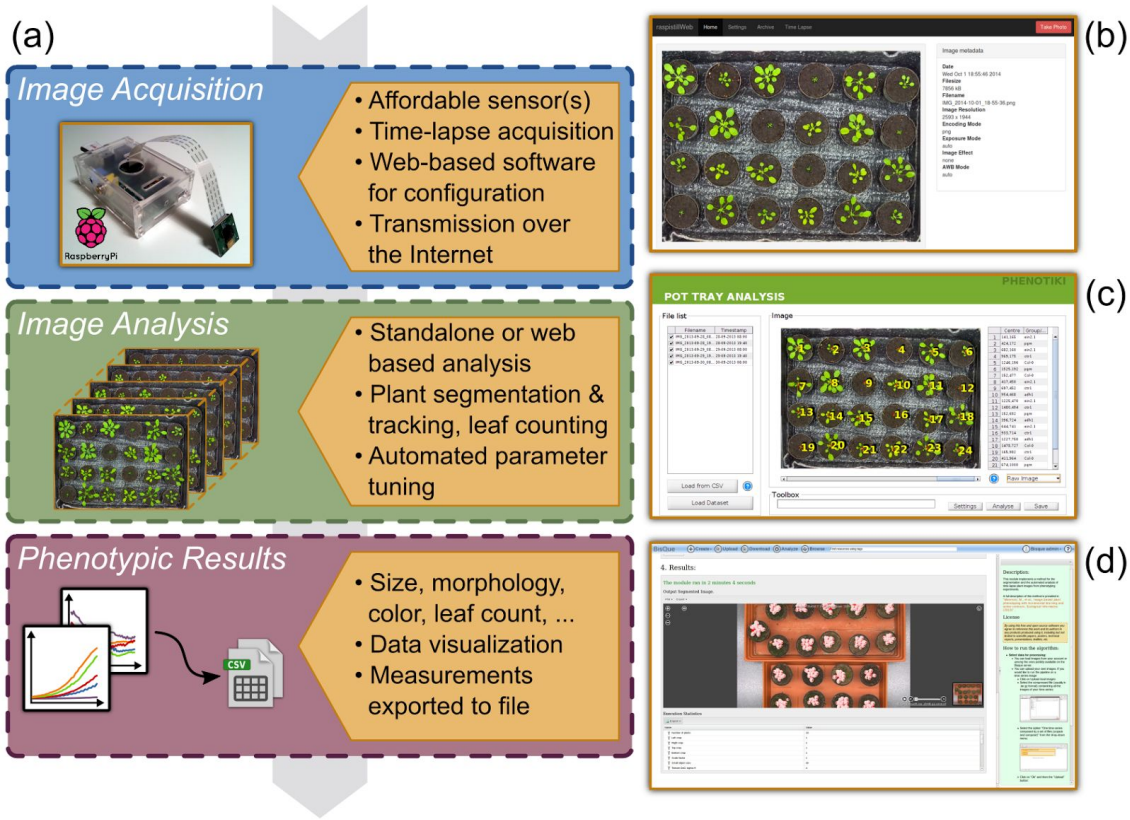
(a)
Image Acquisition
• Affordable sensor(s)
• Time-lapse acquisition
• Web-based software for configuration
• Transmission over the Internet
RaspberryPi
Image Analysis
• Standalone or web based analysis
• Plant segmentation & tracking, leaf counting
• Automated parameter tuning
Phenotypic Results
CSV
• Size, morphology, color, leaf count, ...
• Data visualization
• Measurements exported to file
(b)
(c)
POT TRAY ANALYSIS
PHENOTIKI
(d)

Figure 2

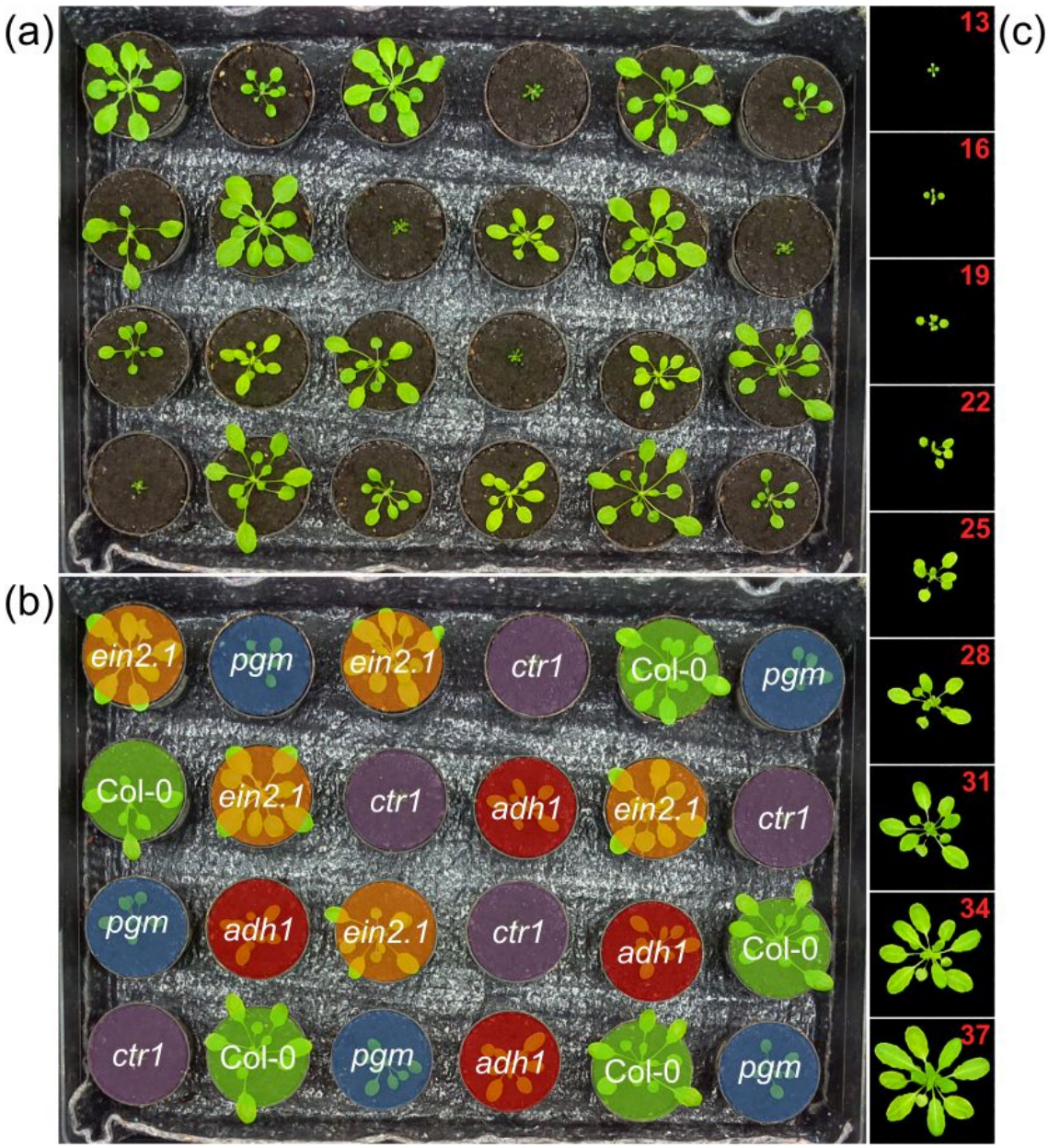
(a)
(b)
(c)
ein2.1
pgm
ein2.1
ctr1
Col-0
pgm
Col-0
ein2.1
ctr1
adh1
ein2.1
ctr1
pgm
adh1
ein2.1
ctr1
adh1
Col-0
ctr1
Col-0
pgm
adh1
Col-0
pgm
13
16
19
22
25
28
31
34
37

Figure 3

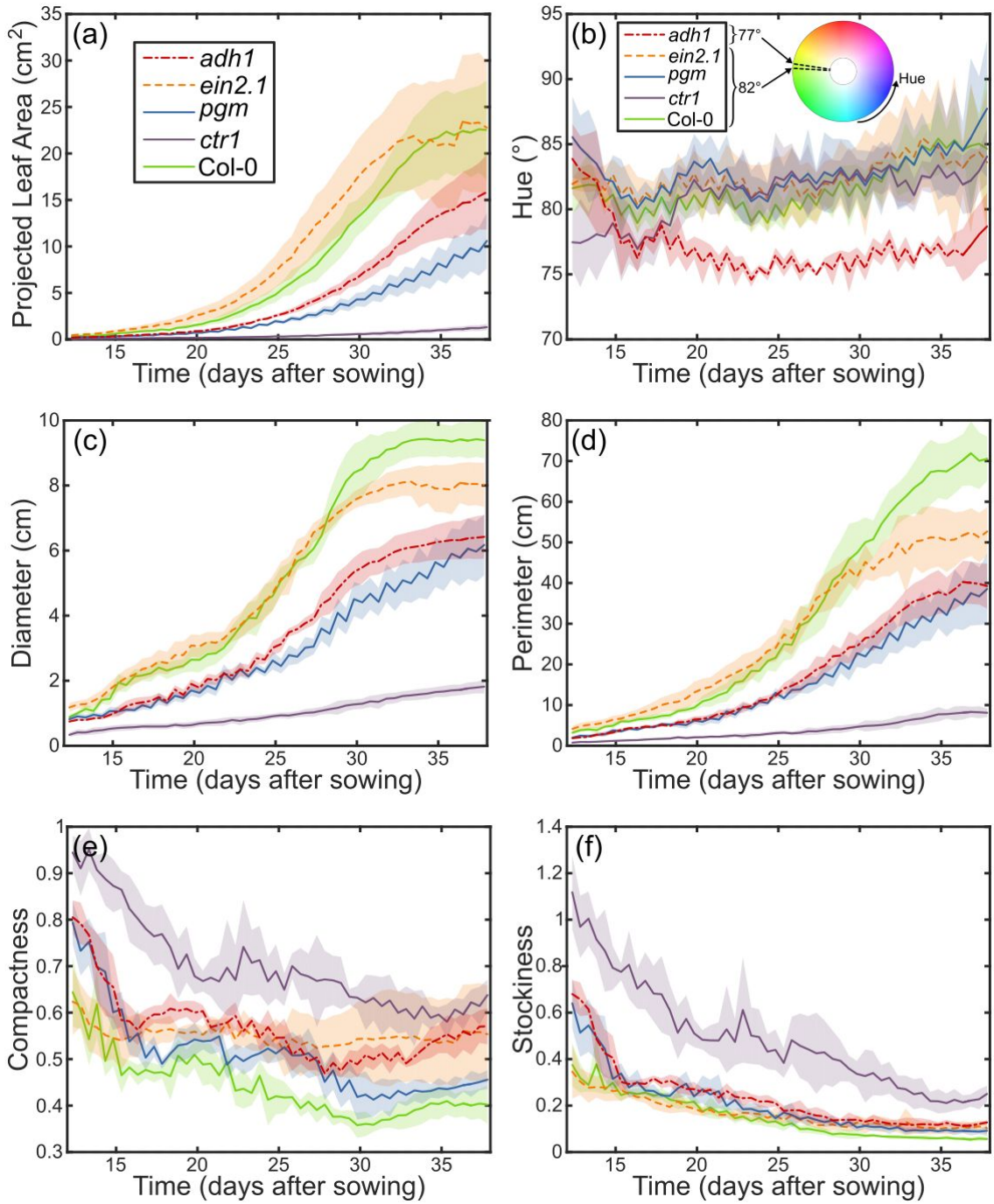
(a)
Projected Leaf Area (cm²)
adh1
ein2.1
pgm
ctr1
Col-0
Time (days after sowing)
(b)
Hue (°)
77°
82°
Hue
Time (days after sowing)
(c)
Diameter (cm)
Time (days after sowing)
(d)
Perimeter (cm)
Time (days after sowing)
(e)
Compactness
Time (days after sowing)
(f)
Stockiness
Time (days after sowing)

Figure 4

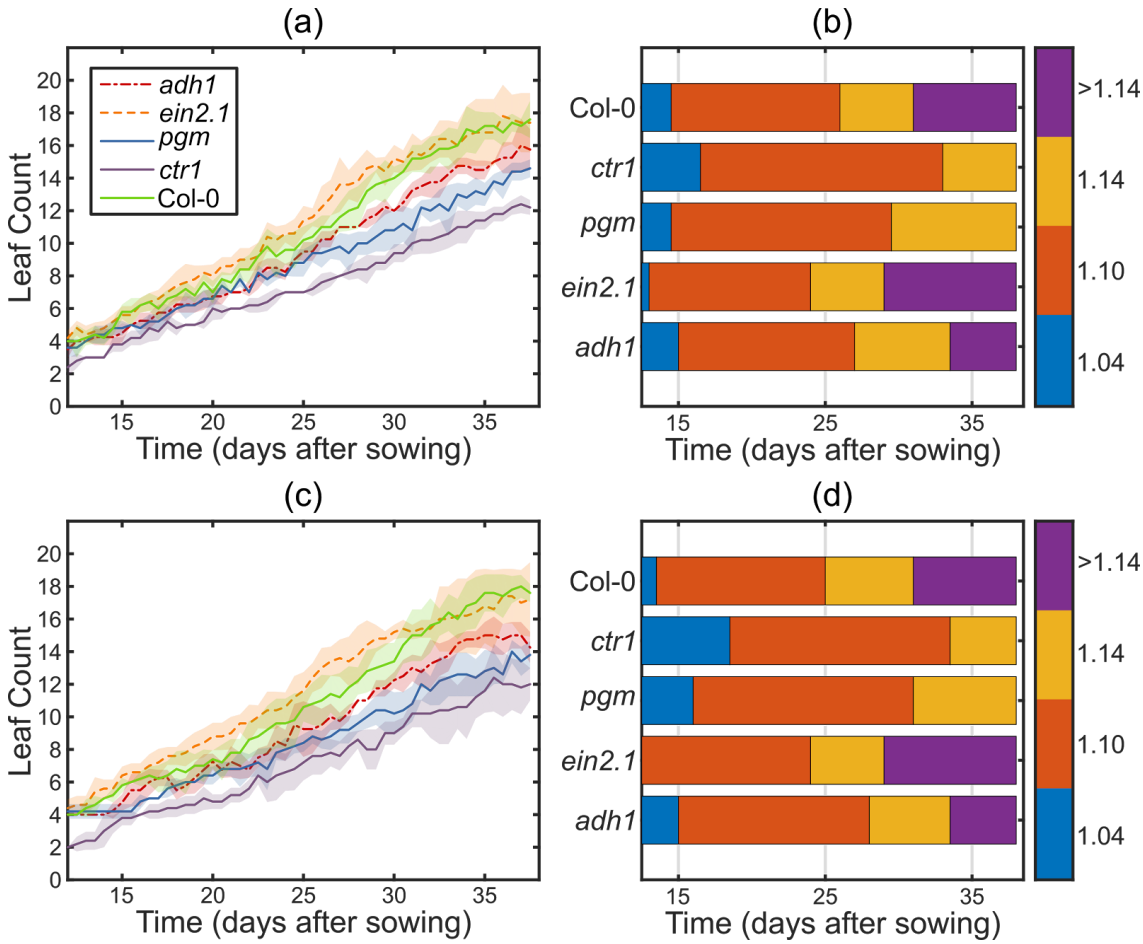
(a)
(b)
(c)
(d)
adh1
ein2.1
pgm
ctr1
Col-0
Leaf Count
Time (days after sowing)
>1.14
1.14
1.10
1.04

Figure 5

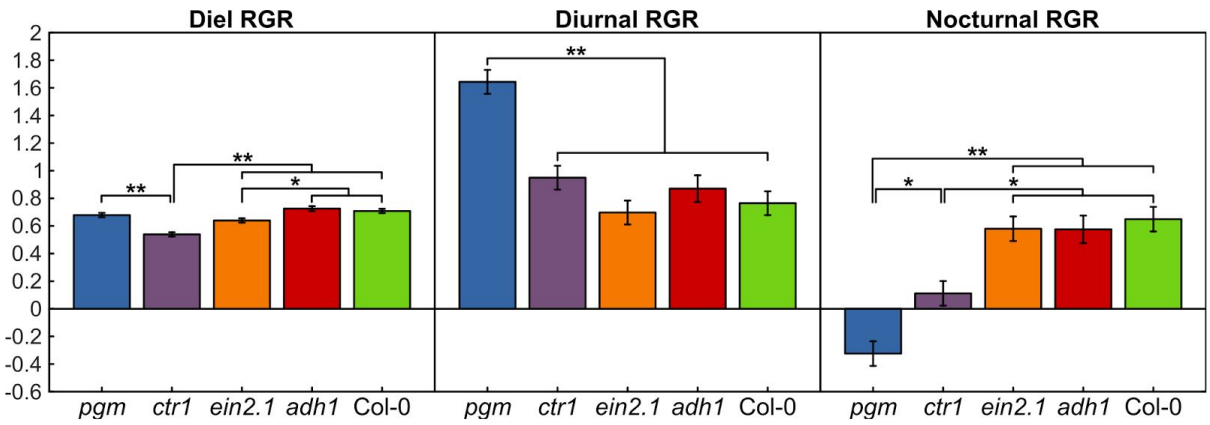
Diel RGR
Diurnal RGR
Nocturnal RGR
2
1.8
1.6
1.4
1.2
1
0.8
0.6
0.4
0.2
0
-0.2
-0.4
-0.6
**
**
*
**
*
**
*
pgm
ctr1
ein2.1
adh1
Col-0

Figure 6

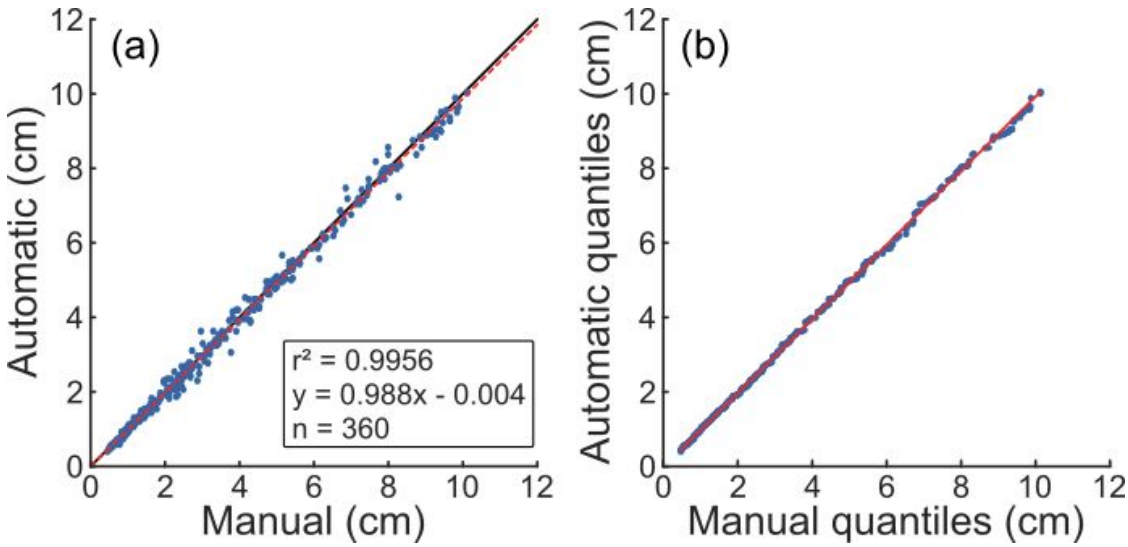
(a)
Automatic (cm)
Manual (cm)
r² = 0.9956
y = 0.988x - 0.004
n = 360
(b)
Automatic quantiles (cm)
Manual quantiles (cm)

Table 1. Quantitative performance of the leaf counting algorithm in Phenotiki. We compared the original algorithm in (Giuffrida et al., 2015) and the extended version proposed in this article. Difference in count (*DiC*), absolute difference in count (|*DiC*|), mean squared error (*MSE*), and coefficient of determination (R^2). Lower *DiC*, |*DiC*|, and *MSE* are better, whereas higher R^2 is better. The best results are highlighted in bold.

	Phenotiki		Giuffrida et al., 2015	
	Training	Testing[$]	Training	Testing
DiC	**0.032 ± 0.772**	**0.186 ± 0.995**	0.107 ± 1.171	0.247 ± 0.1.428
|*DiC*|	**0.580 ± 0.509**	**0.702 ± 0.728**	0.880 ± 0.779	1.048 ± 1.000
MSE	**0.596**	**1.022**	1.380	2.096
R^2	**0.967**	**0.939**	0.926	0.876

Note: These numbers, following typical practice in machine learning literature, reflect performance under a random sampling of the sets that we train on and test on. We follow a strict subject-out 50% split of the complete data. The dataset includes 24 plants imaged for 26 days. The dataset is split in two halves, randomly selecting each time 12 plants (and all the pictures of a plant across time) as training set and the remaining 12 as testing set (used to assess generalization error), ensuring that both subsets include examples of all genotypes (Col-0, *adh1*, *ctr1*, *ein2.1*, and *pgm*). Hence the values of *DiC* and |*DiC*| reflect average and standard deviation on each set; whereas *MSE* and R^2 are by definition aggregates.

[$] If we are to repeat this random split many times (in machine learning this is a form of cross-validation) we see that performance remains the same with average and standard deviations of the same measurements as 0.041±0.154 (*DiC*), 0.841±0.067 (|*DiC*|), 1.335±0.180 (*MSE*), 0.923±0.008 (R^2). This indicates stability w.r.t. the set that we train on.

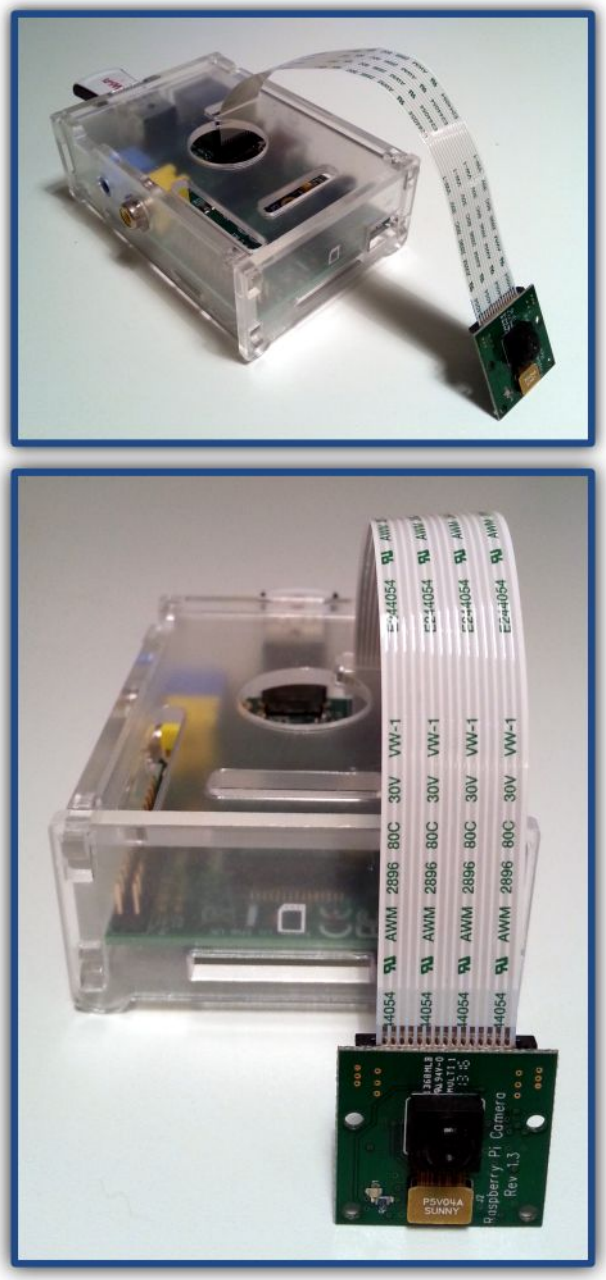

Figure S1. The affordable sensing device adopted in the Phenotiki platform for image-based phenotyping in a box. The main elements of this compact device are the Raspberry Pi single-board computer and the RaspiCam camera sensor. The device is shown here with a non-waterproof/non-humidity resistant enclosure which was used during testing and development and with the imaging sensor (RaspiCam) outside the housing to illustrate the dimensions of the device. An air-tight enclosure with attachment ports is under development.

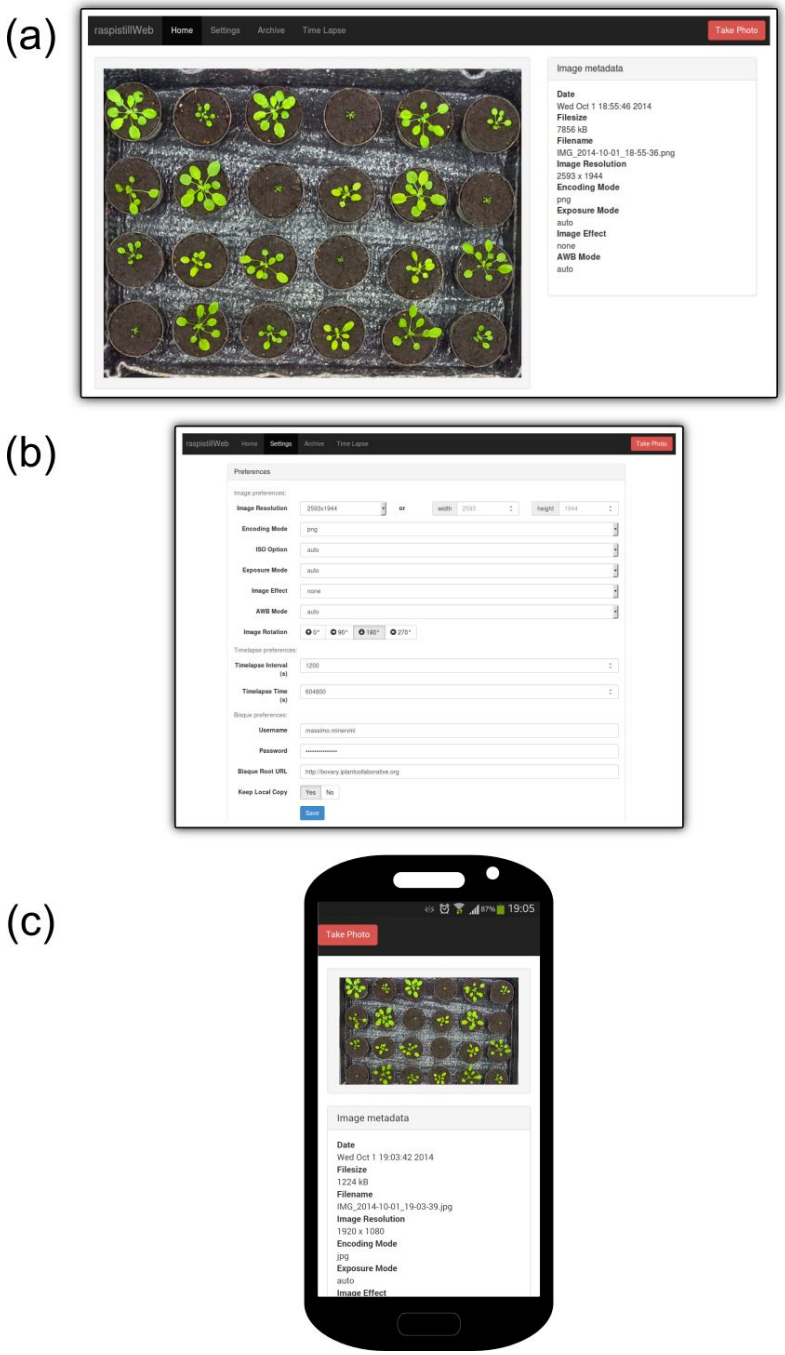

Figure S2. Screen captures of our web-based software tool to easily configure and operate the Phenotiki device from a browser. Our implementation is based on the open source project *raspistillWeb* (https://github.com/TimJuni/raspistillWeb) and the Python programming language. The layout of the graphical interface adapts well to a wide range of viewing environments, therefore the software can be used from (a, b) a desktop computer or (c) a smartphone.

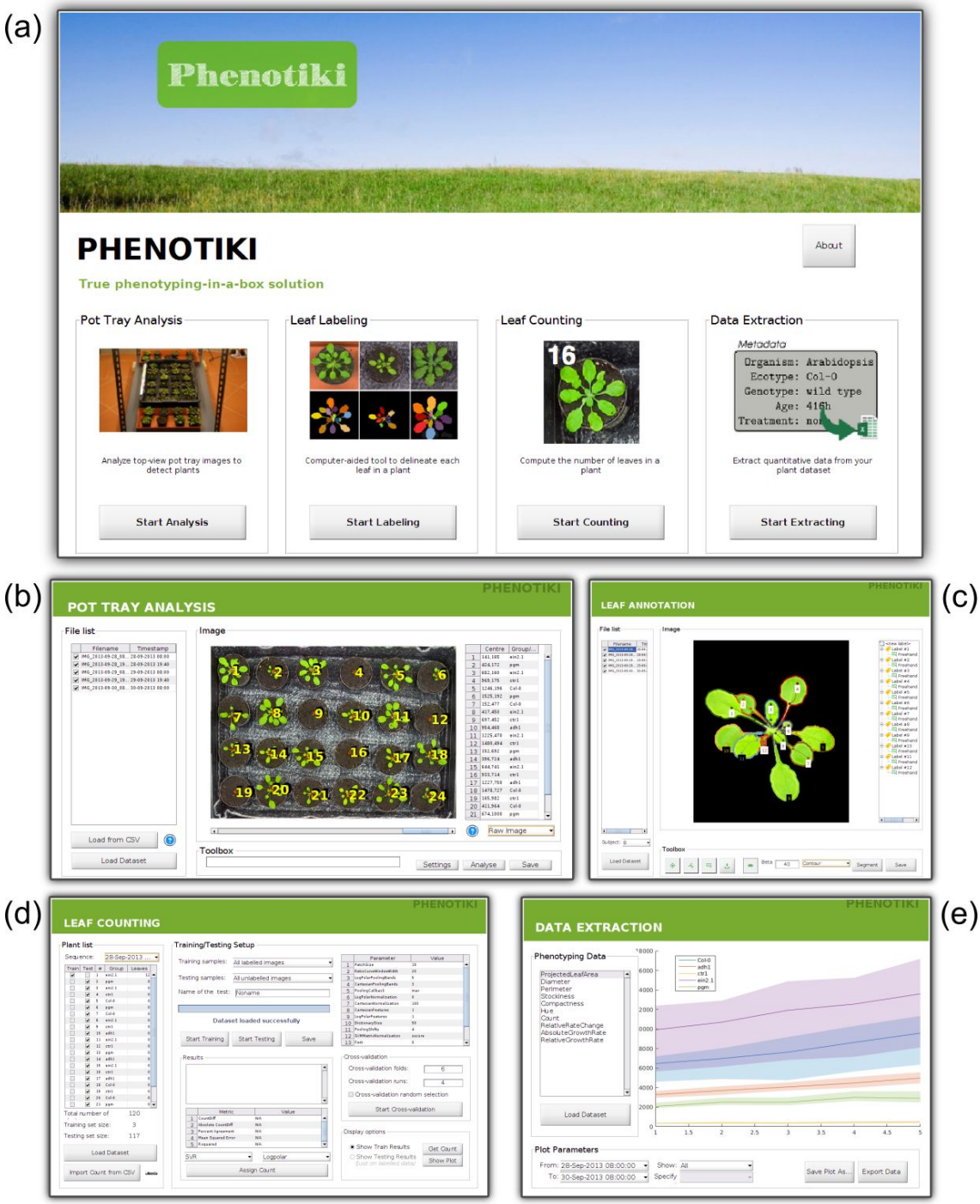

Figure S3. Screen captures of our stand-alone plant image analysis software based on MATLAB. (a) Initial menu showing available modules. (b) Segmentation and tracking of plants in the scene. (c) Semi-automated leaf annotation tool. (d) Automatic leaf counting. (e) Visualization of the results.

Figure S4. Screen captures of our suite of web-based applications for plant image analysis on the CyVerse cloud platform. (a) Example of manual annotation of a plant in an image. (b) Graphical interface to configure parameter optimization and the values reported after execution. (c) Tray image with overlaid segmentation mask found algorithmically and execution statistics.

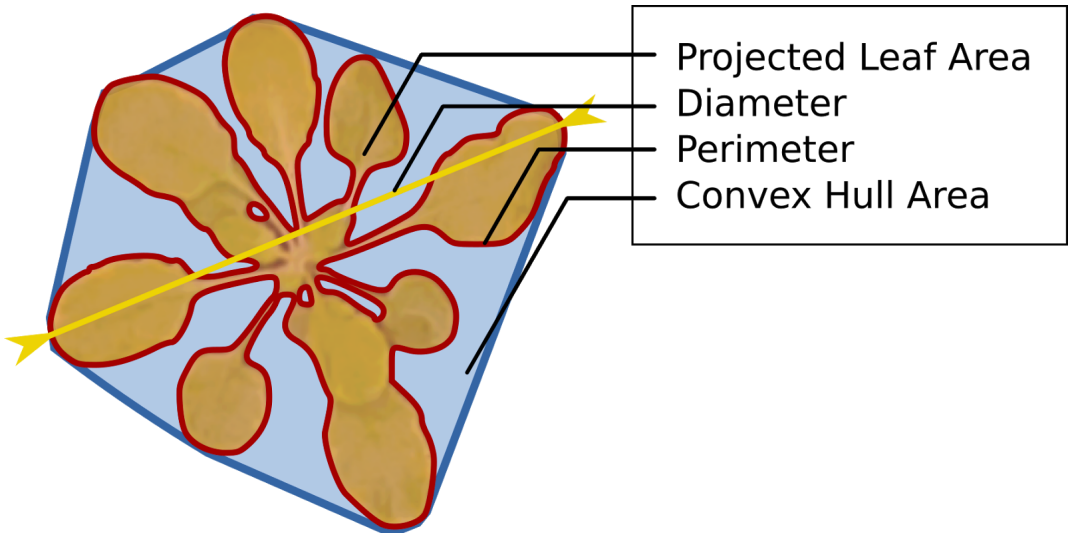

Figure S5. Image of an example Arabidopsis plant illustrating some of the visual traits common in the phenotyping literature extracted by our system.

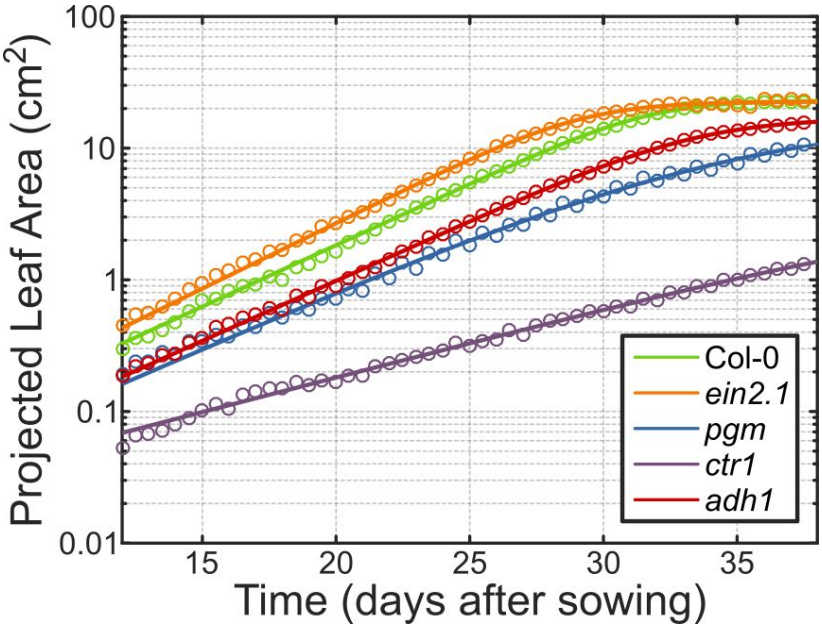

Figure S6. Richards' growth model fitted to average PLA data of each genotype (estimated curve parameters are reported in Table S1). The vertical axis (PLA) is plotted on a logarithmic scale.

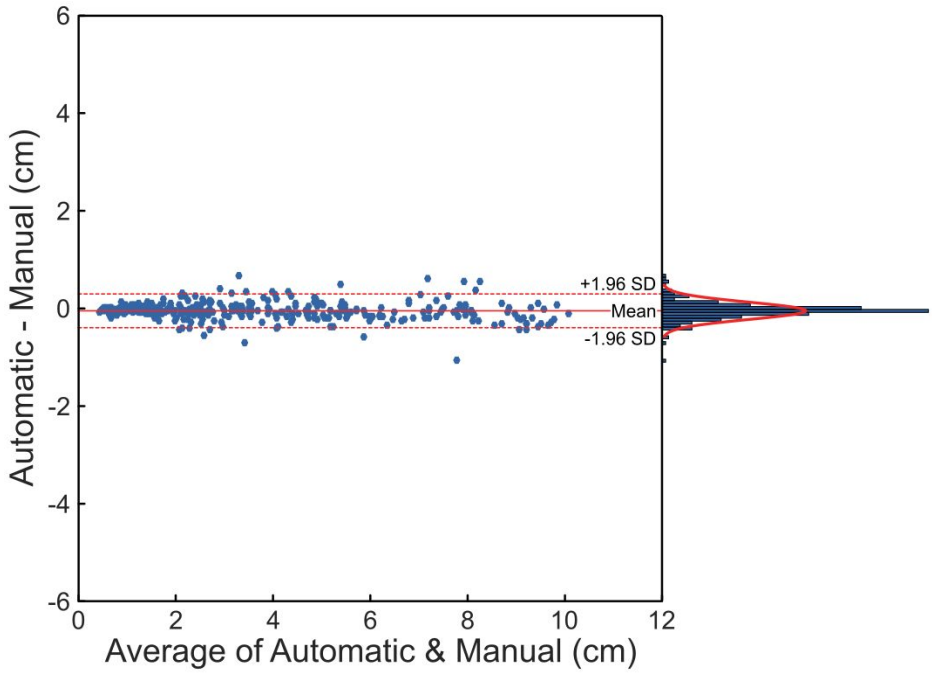

Figure S7. Agreement between rosette diameter measured automatically by Phenotiki (Automatic) and manually with a caliper (Manual). A Bland-Altman plot is shown with the red solid line indicating the bias (mean difference) at -0.048 cm and the red dashed lines indicating the 95% limits of agreement (mean±1.96SD) for repeated measures (Bland and Altman, 2007) at -0.394 and 0.298 cm, respectively. The histogram shows the distribution of differences peaking around the mean (excess kurtosis = 5.2) with superimposed a fitted normal distribution, indicating that in most cases an almost perfect agreement (zero difference) between Automatic and Manual is obtained.

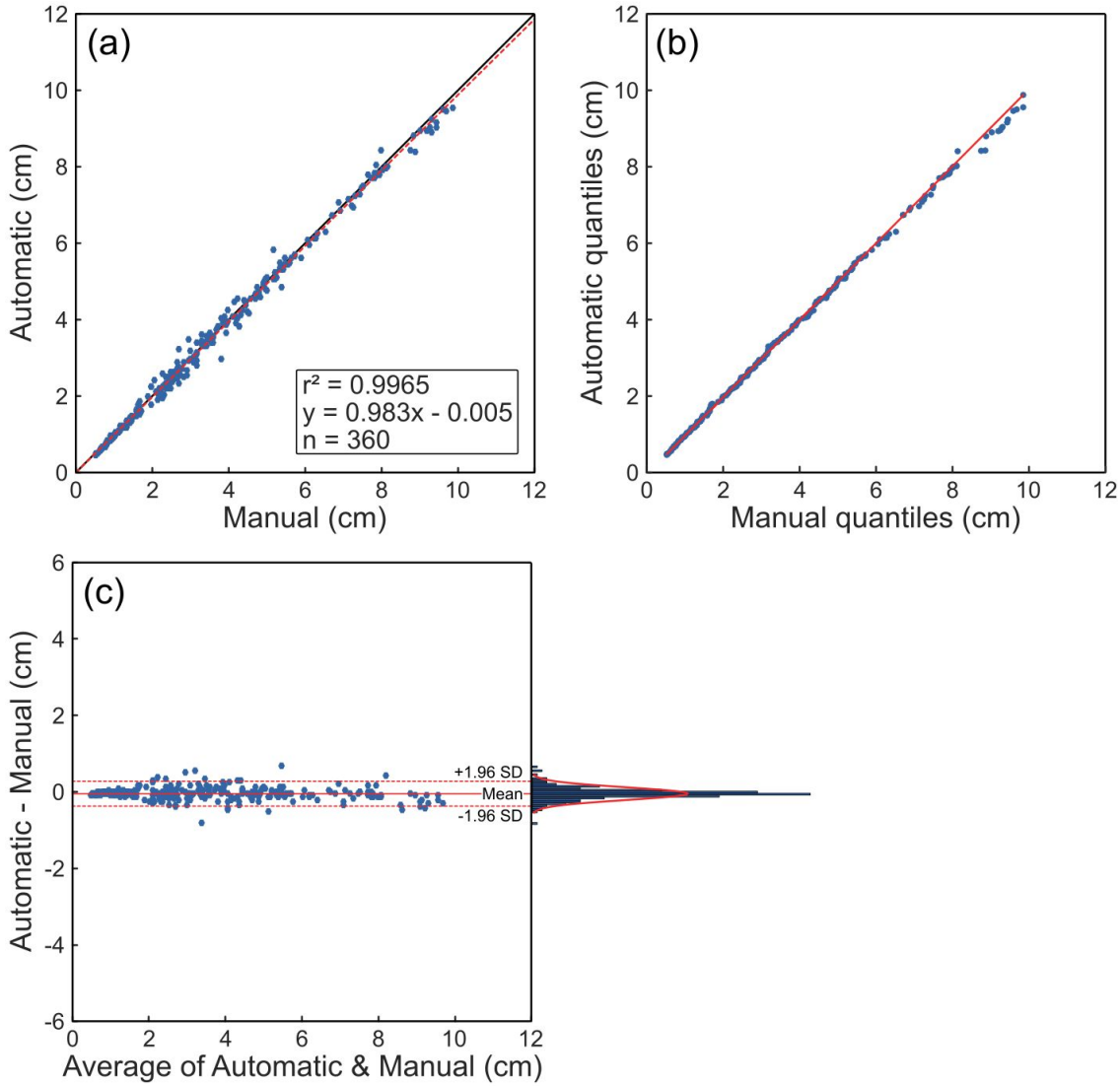

Figure S8. Agreement between rosette diameter measured automatically using the Phenotiki software and images acquired with a Canon camera (Automatic) and manually with a caliper (Manual). This camera has movable optics and can zoom in with a field of view restricted to the size of the tray. It was used to assess the influence of resolution on accuracy. (a) Scatterplot with fitted linear regression (dashed red line) and 45° rising line (black solid line). (b) Q-Q plot with superimposed a red line joining the first and third quartiles of each distribution. (c) Bland-Altman plot with the red solid line indicating the bias (mean difference) at -0.067 cm and the red dashed lines indicating the 95% limits of agreement (mean±1.96SD) for repeated measures (Bland and Altman, 2007) at -0.382 and 0.247 cm, respectively. The histogram shows the distribution of differences peaking around the mean (excess kurtosis = 5.8) with superimposed a fitted normal distribution. Comparing to Figure S7, we see no statistically discernible difference between the bias and limits of agreement of the RaspiCam of Phenotiki with respect to the same gold-standard (manual measurements).

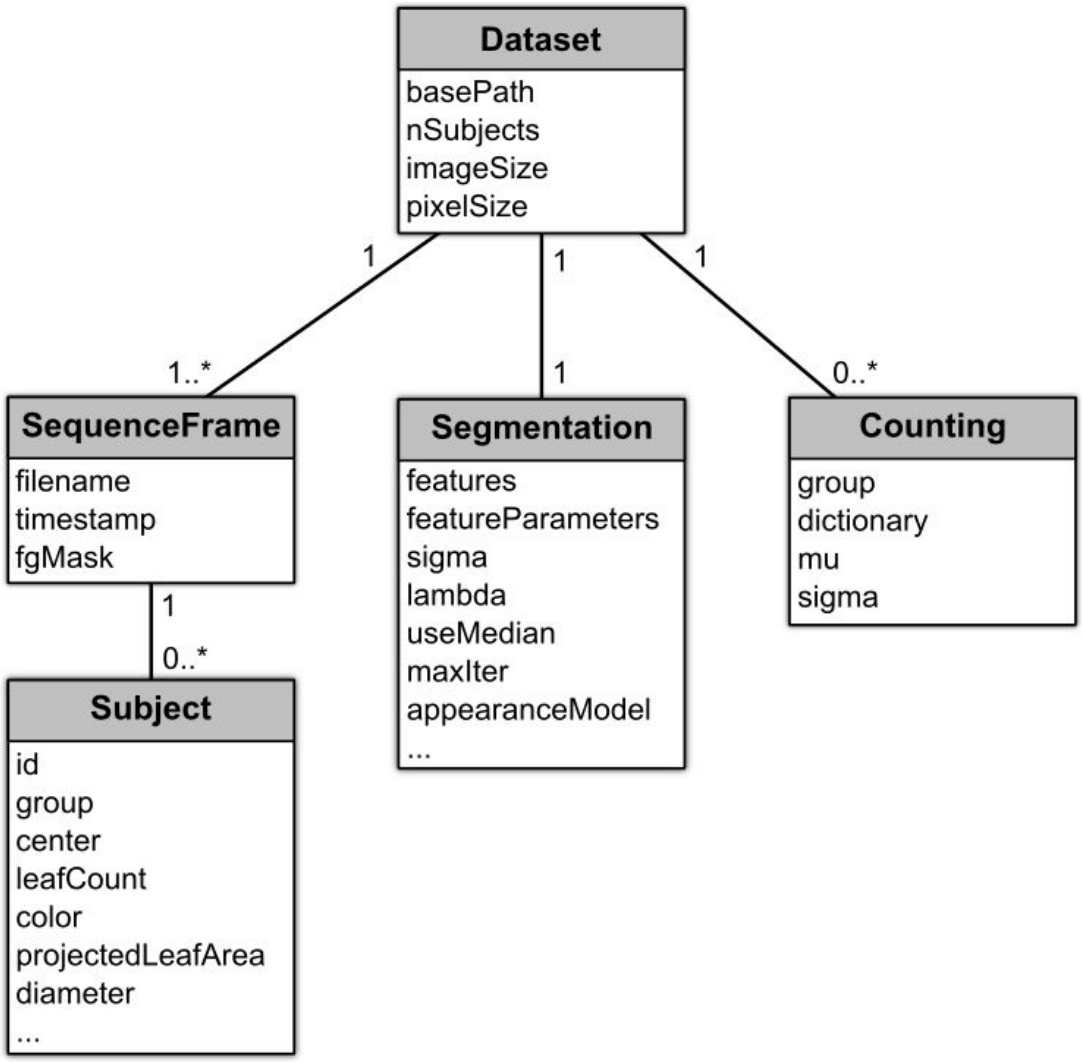

Figure S9. Logical data model used to represent the information associated with an experiment. This conceptual model illustrates the actual data structure used in the Phenotiki software, which is stored in a MAT-file and shared among the analysis modules. The formalism adopted in the diagram is based on the Unified Modeling Language (UML, http://www.uml.org/).

Table S1. Parameter estimates of the Richards' growth curve fitted to PLA data of each genotype, with 95% confidence intervals for the predicted parameters (expressed as lower limit, upper limit).

	L		*k*		γ		δ	
	Est.	95% CI	Est.	95% CI	Est.	95% CI	Est.	95% CI
Col-0	23.04	22.78, 23.29	0.59	0.54, 0.64	30.4	30.25, 30.54	3.74	3.42, 4.06
ein2.1	22.57	22.15, 22.99	0.55	0.45, 0.65	28.01	27.64, 28.38	3.38	2.76, 3.99
pgm	17.65	7.55, 27.75	0.18	0.03, 0.33	35.8	31.86, 39.75	1.89	0.88, 2.91
ctr1	3.39	-3.17, 9.97	0.20	-0.15, 0.55	41.99	23.56, 60.42	2.61	-0.45, 5.68
adh1	16.94	16.47, 17.41	0.44	0.39, 0.49	32.23	32.1, 32.36	3.08	2.77, 3.38

Table S2. Statistical significance of differences in PLA between genotypes is not affected by using the proposed affordable imaging sensor. Shown is the pairwise post-hoc comparison with the Tukey-Kramer method between PLA data of Col-0 and the other genotypes, following a two-way repeated measure ANOVA testing once on RaspiCam derived data and once on Canon data, separately. No difference in the significance of the tests is observed between results obtained with RaspiCam and Canon image sensors, respectively. Sample size (24 subjects, 48 time points) is equal among the two tests.

Genotype (I)	Genotype (J)	Mean Difference	Standard Error	*P*-value	95% Confidence Interval	
					Lower Bound	Upper Bound
RaspiCam						
Col-0	*adh1*	3.9208*	0.9730	0.0057	0.9948	6.8468
	ctr1	8.8514*	0.9174	< 0.001	6.0928	11.6101
	ein2.1	-1.7162	0.9174	0.3653	-4.4748	1.0425
	pgm	5.9184*	0.9174	< 0.001	3.1597	8.6771
Canon						
Col-0	*adh1*	3.6034*	0.9564	0.0101	0.7272	6.4796
	ctr1	8.5434*	0.9017	< 0.001	5.8317	11.2552
	ein2.1	-1.5020	0.9017	0.4768	-4.2137	1.2098
	pgm	5.6314*	0.9017	< 0.001	2.9197	8.3431

* The mean difference is statistically significant at the 0.05 level.

Table S3. Statistical significance of differences in leaf count between genotypes is not affected by using the automated leaf counting module of the Phenotiki analysis software. Shown is the pairwise post-hoc comparison with the Tukey-Kramer method between leaf count data of Col-0 and the other genotypes, following a two-way repeated measure ANOVA testing once on RaspiCam derived data analyzed with Phenotiki and once on manual annotation by an expert, separately. No difference in the significance of the tests is observed between results obtained with Phenotiki and manual annotation, respectively. Sample size (24 subjects, 52 time points) is equal among the two tests.

Genotype (I)	Genotype (J)	Mean Difference	Standard Error	*P*-value	95% Confidence Interval	
					Lower Bound	Upper Bound
Phenotiki						
Col-0	*adh1*	1.1494*	0.3033	0.0096	0.2373	2.0616
	ctr1	3.3240*	0.2860	< 0.001	2.4640	4.1839
	ein2.1	-0.6217	0.2860	0.2315	-1.4817	0.2383
	pgm	1.8529*	0.2860	< 0.001	0.9929	2.7128
Manual						
Col-0	*adh1*	1.3471*	0.3932	0.0209	0.1647	2.5295
	ctr1	3.5962*	0.3707	< 0.001	2.4813	4.7110
	ein2.1	-0.7731	0.3707	0.2664	-1.8879	0.3417
	pgm	2.2423*	0.3707	< 0.001	1.1275	3.3571

* The mean difference is statistically significant at the 0.05 level.

Table S4. Parameter settings used for the Phenotiki leaf counting algorithm. Further details may be found in (Giuffrida et al., 2015). Together with visual features, we added the PLA and the plant's genotype. SVR parameters {C, ɣ, ε} were found using a logarithmic grid search.

Parameter	Description	Value
Patch size	Size of the window used to extract square patches from the images	19×19 pixels
Log-polar pooling area	Width of the window where features are pooled together	5
Log-polar normalization	Rescaling policy of the plant before patches are extracted in order to ensure that patches contain always a plant portion of the same size. If set to dynamic this corrects for different plant sizes but does lose this important plant characteristic. This is compensated by adding the PLA as an additional regressor.	Dynamic
SVR loss parameter (C)	Support Vector Regression (SVR) soft-margin parameter	100
SVR kernel gamma parameter (ɣ)	Gaussian spread parameter of the kernel function	0.0003
SVR error tolerance parameter (ε)	Amount of error allowed by the predictor	1

Methods S1

Hardware: To implement and setup the Phenotiki device we used the following hardware equipment:

- Raspberry Pi 1 Model B; (*)
- Raspberry Pi case; (*)
- RaspiCam camera module; (*)
- USB WiFi dongle; (*)
- 5V micro USB power supply;
- 8 GB Secure Digital (SD) memory card;
- computer monitor and High-Definition Multimedia Interface (HDMI) cable;
- self-powered USB hub;
- USB keyboard;
- USB mouse.

Operating system and specifications: Our Phenotiki device software has been developed and tested on the Raspberry Pi operating system Raspbian "Jessie" version 2015-09-24.

(*) Note that as of May 2016 there is a new version of this model as Raspberry Pi 3 Model B and a new higher resolution camera module (RaspiCam V2). The new model has higher computational power and capabilities, includes built in WiFi (making the USB dongle unnecessary), at the same cost. It is also smaller so it fits in more cases. While the results obtained for this paper were based on the older model and operating system, we have updated the software (of the sensor) to work on the newer operating system.

Methods S2

We devised two implementations of our image analysis software, one for standalone use on a desktop computer and another for web-based use (i.e., via a browser) on the CyVerse cloud. Both versions offer an easy-to-use graphical user interface, encapsulating MATLAB implementations of the underlying image analysis (computer vision) and machine learning algorithms in a modular fashion.

Such common code base has been designed and implemented following the object-oriented paradigm. This choice has the advantages of increasing code modularity, which in turn facilitates maintenance (e.g., releasing updated versions of existing modules) and extension (e.g., developing new analysis modules).

Standalone Version of the Phenotiki Software

Our standalone desktop implementation was developed in MATLAB and is available for download at http://phenotiki.com. Currently, it features four modules: (i) pot tray analysis, (ii) plant/leaf annotation, (iii) leaf counting, and (iv) results visualization. The modules share information on the experiment via a common data structure saved in a MAT-file (see Figure S9). Usage is demonstrated in Movie S2.

Pot tray analysis. Module to detect and segment plants from time-lapse images including multiple plants. This module first localizes and isolates plants within a tray image and then automatically delineates plant objects from the background (e.g., soil, tray), requiring minimal user interaction such as approximate plant locations (provided via mouse clicks) and few additional parameters. To relieve the user from manually tuning such parameters by trial and error, our system is able to optimize them automatically for a specific setup based on user feedback. The user annotates manually foreground (plant) and background regions in one or more images (see annotation tool below) and our software will search for the parameters that ensure best plant segmentation performance on this training dataset (based on overlap criteria between manual and automatic segmentations). With suitable parameters known, the user can launch the batch analysis of a dataset, from which visual phenotypes will be extracted. Note that when experimental settings remain the same (same lab, chamber, camera placement) this process is not necessary to be repeated.

Leaf annotation. Module for rapid and semi-automated plant and leaf delineation requiring minimal user interaction. To obtain a plant segmentation, the user provides annotations by drawing freehand lines, respectively, on plant and background. For individual leaf segmentation, the user draws a freehand line (or just clicks) on each leaf.

Further details on methodology and validation of the annotation tool are available in (Minervini et al., 2015a).

Leaf counting. Module to automatically count the number of visible rosette leaves. The learning-based approach (Giuffrida et al., 2015) relies on a model trained from a small set of annotated single-plant images, for which the user inputs the number of leaves. The model is then used to batch process a dataset and estimate leaf count for new plant images.

Results visualization. Module to visualize and export phenotyping data to comma-separated values (CSV) files. This allows the user to perform preliminary analysis within the software, or more complicated ones using external statistical packages, such as SPSS, Stata, or R.

Cloud-based Version of the Phenotiki Software

We also devised a cloud implementation of our plant image analysis software and a web-based graphical user interface on the scientific cloud platform offered by the CyVerse and the BisQue framework (Goff et al., 2011). The software can be accessed at http://bisque.iplantcollaborative.org after signing in with user credentials. Usage is demonstrated in Movie S3.

Our cloud solution is structured as a suite of three web-based applications with a set of functionalities: (i) *PhidiasAnnotate*, permitting manual annotation of images to delineate plant regions; (ii) *PhidiasModel*, offering automated optimization of image analysis algorithm parameters, via a grid search (on the cloud) on a training dataset of images and corresponding plant annotations (obtained e.g. with PhidiasAnnotate); (iii) *PhidiasAnalyse*, permitting batch analysis of a dataset of time-lapse images of plants and also visualization and exportation of the results.

Methods S3

In this supplement, we provide a brief overview of the computer vision approaches adopted in the Phenotiki image analysis software for plant segmentation and leaf annotation (leaf counting is discussed in the manuscript). For a comprehensive description and validation of the image analysis methods we refer the reader to the corresponding papers (Minervini et al., 2014; Minervini et al., 2015a) that we have published in technical journals and conferences.

Plant Segmentation

To accurately delineate plant objects from the background in time-lapse images, we adopted a vector-valued active contour algorithm based on a level set formulation that incorporates features of color intensity, local texture, and prior knowledge (Minervini et al., 2014). Prior knowledge was introduced to render our solution adaptable to a variety of different settings, and abstract it from a specific setup or plant species. We incorporated the prior on plant appearance using a Gaussian mixture model that learns iteratively the visual appearance of plants, based on information from previously segmented instances or user feedback. We validated our approach on Arabidopsis: comparisons with manual delineations showed that the proposed method can deal with images with complicated and changing background in an automated fashion, offering higher accuracy than other state-of-the-art approaches (Minervini et al., 2014).

Semi-Automated Leaf Annotation

The annotation tool can be used to semi-automatically segment leaves in images of rosette-shaped plants (Minervini et al., 2015a). The graphical interface allows the user to interactively provide annotations (at least one per leaf) in the form of a dot, a line segment, or a scribble (i.e., a freehand line). Subsequently, relying on a graph-based segmentation algorithm, the annotations are propagated to the rest of the image until leaf boundaries are reached (the background can be eliminated by first using the plant segmentation module). The resulting leaf segmentation mask (obtained in few seconds) contains a partitioning of the image pixels into distinct leaf regions, which can be used to extract leaf-level phenotypic information (e.g., individual leaf area or orientation for fine-grained growth analysis) or to obtain annotated data to train learning-based algorithms, such as the Phenotiki leaf counting module. The tool has been validated on images of Arabidopsis and tobacco (Minervini et al., 2015a). Using scribble annotations on average almost 97% overlap agreement was obtained with respect to leaf delineations drawn by an expert in a completely manual fashion –a highly time-consuming task.

Methods S4

In order to express the visual phenotype of Arabidopsis quantitatively, we extracted the following plant trait descriptors (some of which are visually depicted in Figure S5).

- *Projected Leaf Area* (PLA): area of the plant calculated as the number of visible plant pixels in the image, expressed in cm^2.
- *Diameter*: the longest distance between any two points on the boundary of the plant, expressed in cm.
- *Perimeter*: perimeter of the rosette calculated as the number of boundary pixels, expressed in cm.
- *Compactness* (or solidity):

  $$Compactness = \frac{PLA}{A_{CVX}}$$

  where A_{CVX} is the area of the smallest convex region (hull) enclosing the plant. Value of 1 reflects a perfectly solid object; less than 1 for irregular boundaries or holes.

- *Stockiness* (or form factor):

  $$Stockiness = \frac{4\pi A}{P^2}$$

  where A and P denote, respectively, PLA and perimeter. Stockiness ranges between 0 and 1, where 1 denotes a perfectly circular object.
- *Leaf count*: number of visible plant leaves.
- *Relative Growth Rate* (RGR):

  $$RGR = \frac{\log A_2 - \log A_1}{t_2 - t_1}$$

  where A_1 and A_2 denote PLA measured at two time instants, respectively, t_1

and t_2. RGR (%h^{-1}) measures plant growth between consecutive time instants and is robust to initial differences in size among subjects.

- *Color*: average intensity of the hue component (H) of the HSV (Hue, Saturation, Value) color space, which can represent color information with some invariance to illumination changes. Hue is measured in degrees, in the range 0 to 360°, and is visually depicted by the color wheel in Figure 3b.

Methods S5

To model variation in time of Projected Leaf Area (PLA), used here as a proxy for plant biomass, we adopted the following form of generalized logistic function known as Richards' curve:

$$y(t) = L(1 + (\delta - 1)e^{-k(t-\gamma)})^{\frac{1}{1-\delta}},$$

where $y(t)$ denotes PLA at time t, L is the upper asymptote, k is the growth rate, γ is the point of inflection on the x-axis, and δ affects near which asymptote maximum growth occurs. PLA at the time of inflection γ is $L\delta^{1/(1-\delta)}$. Average normalized growth rate for Richards' curve is defined as $k/2(\delta + 1)$.

We estimated the parameters L, k, γ, and δ of Richards' curve for PLA data using a trust region algorithm for nonlinear least-squares fitting with a positivity constraint on parameter values (estimated coefficients are reported in Table S1).

Results S1

To investigate the presence of cyclic patterns in growth data we adopt an exploratory data analysis tool routinely used in signal processing. The figure below shows the spectral characteristics of PLA temporal data for each genotype, obtained with Thomson's multitaper power spectral density estimation. Col-0, *adh1*, and *ein2.1* present only one major peak at a very low frequency, corresponding to the fundamental increasing trend of PLA in time. On the other hand, *pgm* presents also a second prominent frequency component close to 1 cycle/day. The plants were imaged twice per day every 12 hours, thus a cycle that takes one day to complete suggests different diurnal and nocturnal growth behaviors. A similar observation can be made for *ctr1*, although the peak at the same 1 cycle/day frequency is less evident.